

P-1689



Analysis of Fuel Flow in Fuel Cell for Efficient Power Generation



A Project Report

Submitted by

V.Balaji - 71204402001



*in partial fulfillment for the award of the degree
of*

Master of Engineering
in
CAD/CAM

**DEPARTMENT OF MECHANICAL ENGINEERING
KUMARAGURU COLLEGE OF TECHNOLOGY
COIMBATORE - 641 006**

ANNA UNIVERSITY:: CHENNAI 600 025

APRIL- 2006

ANNA UNIVERSITY :: CHENNAI 600 025

BONAFIDE CERTIFICATE

Certified that this project report entitled "Analysis of Fuel Flow in Fuel Cell for Efficient Power Generation" is the bonafide work of

Mr. V.Balaji

Register No. 71204402001

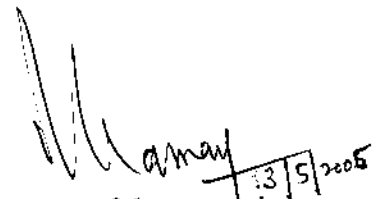
Who carried out the project work under my supervision.



Signature of the HOD

Dr. T. P. MANI

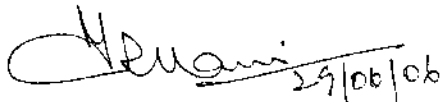
HEAD OF THE DEPARTMENT



Signature of the supervisor

Mr. T.KANNAN

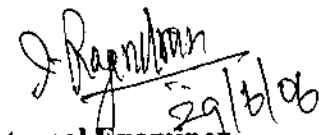
ASSISTANT PROFESSOR



Internal Examiner

Dr. T.P. Mani

B.E. M.E. Ph.D. DML., MIE. MNQR., MISTE.,
Dean & HoD / Dept. of Mech. Engg.
Kumaraguru College of Technology
Coimbatore - 641 006



External Examiner

DEPARTMENT OF MECHANICAL ENGINEERING
KUMARAGURU COLLEGE OF TECHNOLOGY
COIMBATORE 641 006



National Conference on
Optimization Techniques in Engineering Sciences and Technologies

OPTEST - 2006



RWTTUV

held at
BANNARI AMMAN INSTITUTE OF TECHNOLOGY


Sathyamangalam-638 401 during
April 11-12, 2006

Certificate


This is to certify that Mr./Ms./Mrs **V. Balaji**
has participated / presented a paper entitled **ANALYSIS OF FLUID FLOW IN FUEL CELL**

..... **FOR EFFICIENT POWER GENERATION**

in the National Conference on "Optimization Techniques in Engineering Sciences and Technologies (OPTEST-2006)" during 11-12 April 2006, organized by the Department of Mechanical Engineering, Bannari Amman Institute of Technology, Sathyamangalam.


C SASIKUMAR/ G SASIKUMAR
Organizing Secretaries


Dr K THIRUNAVUKKARASU
Convener


D/A SHANMUGAM
Chairman

ABSTRACT

These days' fuel cells are playing an important role in power generation. Fuel cell is an electrochemical device, which directly converts chemical energy stored in a fuel (hydrogen) and an oxidizer (oxygen) into electrical energy. In this work, PEM (Polymer Electrolyte Membrane) electrolyte has been used to analyse the fluid flow in the fuel cell to increase the power generation.

A mathematical model is developed to analyze for proper fuel flow and to get more efficiency. Graphs are plotted for various input conditions. From the result best-input conditions are taken. Using the mathematical model results flow rate, pressure, temperature and velocity are examined. Optimal conditions are found for maximum electric power generation. Optimal conditions are making the life of the fuel cell longer with the little loss of power generation performance in fuel cell.

Geometric model has been developed for the given dimensions and the model is meshed using GAMBIT. Model is imported in FLUENT and the results are obtained for the geometric model. Pressure, velocity and temperature distribution with in the Fuel cell are presented in graphical form.

ஆய்வுச் சுருக்கம்

இந்நாட்களில் எரிபொருள் மின்கலமானது மின்சாரம் தயாரிப்பதில் முக்கியப் பங்கு வகிக்கிறது. எரிபொருள் மின்கலமானது ஒரு மின்வேதியியல் கருவி, இது எரிபொருளில் சேமித்து வைத்துள்ள வேதியாற்றல் மற்றும் ஆக்சிஜனேற்றியை நேரிடையாக மின்னாற்றலாக மாற்றுகிறது. இந்தப் பணியானது ஓட்டபரவல் மற்றும் பயனுறுதிறன் மூலமாக, தரப்பட்ட சூழ்நிலைகளுக்கு மின்சாரம் தயாரிப்பதை அதிகரிக்கிறது. இந்த பணியில் எரிபொருள் மின்கலத்தில் உள்ள திரவ ஓட்டத்தை ஆராய பல்படிச்சேர்ம மின்பகுளி படலமானது (PEM) உபயோகிக்கப்பட்டது.

சீரான எரிபொருள் ஓட்டம் மற்றும் அதிகப்படியான பயனுறுதிறனைப் பெற கணித மாதிரியானது உருவாக்கப்பட்டது. பல்வேறுபட்ட இடுவரல் சூழ்நிலைகளுக்கு வரைபடங்களானது வரைப்பட்டது. இந்த வரைபடங்களின் விளைவுகளிலிருந்து நல்ல இடுவரல் சூழ்நிலைகளானது எடுக்கப்பட்டது. கணித மாதிரியை உபயோகித்து ஓட்ட வீதம், அழுத்தம், வெப்பநிலை மற்றும் திசைவேகமானது ஆராயப்பட்டது. இந்த ஆராய்ச்சியிலிருந்து அதிகப்படியான மின்சாரம் தயாரிப்பதற்குப் போதுமான சூழ்நிலைகள் கண்டறியப்பட்டது. இந்த போதுமான சூழ்நிலைகளானது மின்சாரம் தயாரிப்பதின் செயல்திறனில் சிறிது இழப்பு மூலமாக எரிபொருள் மின்கலத்தின் செயல்காலத்தை அதிகரிக்கிறது.

கொடுக்கப்பட்ட பரிமாணத்திற்கு வடிவக் கணித மாதிரியானது உருவாக்கப்பட்டது. GEMBIT மற்றும் FLUENT மென் பொருள்களைப் பயன்படுத்தி, இந்த எரிபொருள் மின்கலம் வடிவமைக்கப்பட்டு ஆராய்ச்சி மேற்கொள்ளப்பட்டது. ஆராய்ச்சியின் மூலம் வடிவக்கணித மாதிரியின் விளைவுகளானது பெறப்பட்டது, விளைவுகளின் விளக்கப்படமானது எரிபொருள் மின்கலத்தின் அழுத்தம், திசைவேகம், மற்றும் வெப்பநிலை பரவல்களை காட்டுகிறது.

ACKNOWLEDGEMENT

The author grateful to his guide **Mr.T.Kannan**, Assistant Professor, Department of Mechanical Engineering, Kumaraguru College of Technology, Coimbatore for his excellent, utmost motivation, valuable advice, untiring support, timely suggestion, constant encouragement, enthusiasm, relentless patience, and inspiration throughout the study, holding in all the places.

The author expresses humble gratitude to **Dr.T.P.Mani**, Head of the Department, Mechanical Engineering, Kumaraguru College of Technology, Coimbatore for facilitating conditions for carrying out the work smoothly.

The author wish to express his deep sense of reverential gratitude to **Dr.K.K.Padmanabhan**, Principal, Kumaraguru College of Technology, Coimbatore, for providing the facilities to conduct this study.

The author expresses his heartfelt thanks to **Dr.N.Gunasekaran**, Professor, Department of Mechanical Engineering, Kumaraguru College of Technology, Coimbatore.

The author also wish to thank **Mr.B.N.Sriharan**, and **Mr.N.Siva Kumar**, Lab Technicians, CAD Lab for being with him throughout this venture, right from the scratch and helping for completing the project successfully.

The author owes his sincere thanks to all elders, parents, teachers and Lord Almighty who have bestowed upon their generous blessings in all endeavors.

CONTENTS

Title	Page No.
Certificate	i
Abstract	iii
Acknowledgement	v
Contents	vi
List of Tables	ix
List of Figures	x
List of Symbols	xi
CHAPTER 1 PROBLEM DEFINITION	1
1.1 Introduction	2
1.2 Over View of Project	3
CHAPTER 2 LITERATURE SURVEY	5
CHAPTER 3 FUEL CELL	12
3.1 Introduction	13
3.2 Types of Fuel cell	14
3.2.1 Phosphoric Acid Fuel Cell	14
3.2.2 Polymer Electrolyte Membrane	14
3.2.3 Molten Carbonate Fuel Cell	15
3.2.4 Solid Oxide Fuel Cell	16
3.2.5 Alkaline	16
3.2.6 Direct Methanol Fuel Cell	17
3.2.7 Regenerative Fuel Cell	17
3.2.8 Zinc-Air Fuel cell	18
3.2.9 Protonic Ceramic Fuel Cell	18
CHAPTER 4 COMPUTATIONAL FLUID DYNAMICS	20
4.1 Introduction	21
4.2 Governing Equations	22
4.2.1 Conservation of Mass	22
4.2.2 Conservation of Momentum	23
4.2.3 The Energy Equation	23

4.3	Program Structure	24
4.3.1	Grid Generation and GAMBIT	25
4.3.2	Boundary Conditions	27
4.3.3	Solution Algorithms	28
4.3.4	Convergences	29
4.3.5	Background of the CFD Solver used (FLUENT)	29
4.4	Basic Elements of CFD	30
4.4.1	Pre-processor	30
4.4.2	Solver	31
4.4.3	Post-processor	31
4.4.4	CFD Simulation	31
4.5	Problem solving Steps	32
CHAPTER 5	MODEL DEVELOPMENT	33
5.1	Introduction	34
5.2	Model Dimensions	34
5.3	Model Description and Field Equations	36
5.3.1	Assumptions	36
5.3.2	Model Equations in Gas Flow Channel	37
5.3.3	Mass Transport Equations	38
5.3.4	Energy Transport	39
5.3.5	Model Equations in Gas Diffusion Layer	39
5.3.6	Mass Transport Equation in Porous Media	40
5.3.7	Energy Transport in Porous Media	41
5.3.8	Potential	41
5.3.9	Catalyst Layer	41
5.3.10	Boundary Conditions	41
5.4	Mathematical Model	44
5.5	Physical Properties and Operating Parameters of PEM Fuel Cell	46
5.5.1	Physical Dimensions	47
5.5.2	Operating Parameters	48
5.5.3	Mass Fraction	48

5.5.4	Electrode Properties	49
5.5.5	Membrane Properties	49
5.6	Graphs	50
CHAPTER 6	MODELING AND INITIAL CONDITIONS	53
6.1	Geometric Modeling	54
6.2	Meshing	55
6.3	Boundary Conditions	56
6.4	Initial Conditions	57
6.5	Grid Check	59
6.6	Iteration Process	60
CHAPTER 7	RESULTS AND DISCUSSIONS	61
CHAPTER 8	CONCLUSIONS	65
REFERENCES		67

LIST OF FIGURES

Figure	Title	Page No.
3.1	Fuel cell	13
4.1	Basic Program Structure	24
5.1	Polymer Electrolyte Membrane Fuel Cell	34
5.2	Cell Configuration for the CFD Model	35
5.3	Relationships between Current Density and Voltage for Different Temperature	50
5.4	Relationships between Current Density, Voltage and efficiency for Different Temperature	51
5.5	Relationships between Current Density, Voltage and efficiency for Different Pressure	52
6.1	Wire Frame Model of Fuel Cell	54
6.2	Partially Meshed Model	55
6.3	Fully Meshed Model	55
6.4	Boundary Conditions	56
6.5	Species Properties	57
6.6	Operating Temperature	58
6.7	Species composition	58
6.8	Reading Mesh File	59
6.9	Grid Check	59
6.10	Scaled Residuals	60
6.11	Iteration Process	60
7.1	Contours of Static Pressure	62
7.2	Density of Fluid in Cell	63
7.3	Density of Fluid in Flow Volume	63
7.4	Velocity	64
7.5	Turbulent Kinetic Energy	64

LIST OF SYMBOLS

E	thermodynamic potential (V)
E^0	standard potential (V)
E_{fc}	thermodynamic efficiency
F	Faraday's constant (96487 C/mol)
i	current density (A/cm^2)
i_0	exchange current density (A/cm^2)
i_l	limiting current density (A/cm^2)
I	current (A)
R	gas constant (8.314 J/mol K)
T	cell temperature (K)
V_{cell}	cell voltage (V)
W_{gross}	gross output power (W)
η_{act}	activation over potential (V)
η_{diff}	diffusion over potential (V)
η_{ohmic}	ohmic over potential (V)
n	number of electrons per reacting ion
LHV_{H_2}	lower heating value of hydrogen (J/kg)
\dot{m}_{H_2}	hydrogen mass flow rate (kg/s)
M_{WH_2}	molecular mass of hydrogen (kg/mol)
P_a, P_c	total pressure of anode and cathode, respectively (atm)
$P_{H_2}, P_{O_2}, P_{H_2O}$	partial pressure of hydrogen, oxygen and water (atm)
$R^{internal}$	total internal area specific resistance (Ωcm^2)
ΔG^0	Gibbs energy change for the reaction under standard conditions (J/mol)

CHAPTER 1

PROBLEM DEFINITION

1.1 INTRODUCTION

Recently, there has been growing concern about acid emissions, carbon dioxide, and other air quality matters, which have made renewable technologies an attractive option. Fuel cell technology is expected to play an important role in meeting the growing demand for distributed generation. In an ongoing effort to meet increasing energy demand and to preserve the global environment, the development of energy systems with readily available fuels, high efficiency and minimal environmental impact is urgently required.

A fuel cell system is expected to meet such demands because it is a chemical power generation device that converts the chemical energy of a clean fuel (e.g., hydrogen) directly into electrical energy. Still a maturing technology, fuel cell technology has already indicated its advantages, such as its high-energy conversion efficiency, modular design and very low environmental intrusion, over conventional power generation equipment.

Among all kinds of fuel cells, Polymer Electrolyte Membrane fuel cells (PEMFCs) are compact and lightweight, work at low temperatures with a high output power density, and offer superior system startup and shutdown performance. These advantages have sparked development efforts in various quarters of industry to open up new field of applications for PEMFCs, including transportation power supplies, compact cogeneration stationary power supplies, portable power supplies, and emergency and disaster backup power supplies. Two key issues limiting the widespread commercialization of fuel cell technology are better performance and lower cost.

PEMFC's performance is limited by polarizations. A good understanding of the effect of design and operating conditions on the cell potential is required in order to reduce polarization. The performance of PEM fuel cells known is to be influenced by many parameters, such as operating temperature, pressure and discharge current. In order to improve fuel cell performances, it is essential to understand these parametric effects on fuel cell operations.

To understand and improve the performance of PEMFC's, researchers have developed several mathematical models to explain the behavior of potential

variation with the discharge current. Mathematical modeling is a powerful tool for improving the performance of fuel cell stacks.

Two main modeling approaches can be found in the literature. The first approach includes mechanistic models, which aim to simulate the heat, mass transfer and electrochemical phenomena encountered in fuel cells. The second approach includes models that are based on empirical equations, which are applied to predict the effect of different input parameters on the voltage-current characteristics of the fuel cell, without examining in depth the physical and electrochemical phenomena involved in fuel cell operation.

Some models are characterized by a high complexity, with several partial differential equations to be taken into account. This high complexity creates problems of simulation times, parameter identifications, etc., especially when they are to be enclosed in a larger system, such as an electric vehicle.

The purpose of this paper, therefore, is to develop a mathematical model for investigating the performance optimization of a PEM fuel cell that, although simplified and containing some semi-empirical equations, is still based on the chemical-physical knowledge of the phenomena occurring inside the cell.

1.2 OVER VIEW OF THE PROJECT

Various peoples over the years have developed different mathematical/numerical models to understand and analyse the phenomena in PEMFC. Except few models, all of them were mainly focused on particular area/processes of the PEMFC. Also the few full models attempted were solved using separate equations governing each region of PEMFC.

But in this project, the model used the single domain approach, in which a single set of governing equations valid for all sub regions is used. The fuel cell operations under isothermal conditions are described by mass, momentum, species and change conservation principles.

The various stages involved in the development of the CFD model and the project as a whole is as follows:

Development of basic governing equations needed for the CFD model. These equations simulate the actual electro-chemical phenomena in the PEMFC

and have been incorporated by several people working in the field of CFD modeling of the different fuel cells as a whole.

The governing equations are discretised using the control-volume based CFD technique and the one-dimensional model is solved by Tri-diagonal Matrix algorithm.

The model is also validated with the calculation procedure to qualify the various parameters in PEMFC for a given power requirement is also incorporated from the results of the CFD model.

CHAPTER 2

LITERATURE SURVEY

alters the current distribution by changing the relative influence of ohmic to activation over-potentials.

Brenda (2004), a one-dimensional, isothermal model for a direct methanol fuel cell (DMFC) is presented. The model accounts for the kinetics of the multi-step methanol oxidation reaction at the anode. Diffusion and crossover of methanol are modeled and the mixed potential of the oxygen cathode due to methanol crossover is included. Kinetic and diffusion parameters are estimated by comparing the model to data from a 25 cm² DMFC. This semi-analytical model can be solved rapidly so that it is suitable for inclusion in real-time system level DMFC simulations. A semi-analytical, one-dimensional, isothermal model of a DMFC has been developed. Using reasonable transport and kinetic parameters the model fits well to experimental polarization data. The model allows prediction of concentration profiles in the anode and membrane as well as estimating methanol crossover.

Kenneth Armstrong (2004), a series of steady-state microscopic continuum models of the cathode catalyst layer (active layer) of a proton exchange membrane fuel cell are developed and presented. This model incorporates O₂ species and ion transport while taking a discrete look at the platinum particles within the active layer. The original 2-dimensional axisymmetric Thin Film and Agglomerate Models of Bultel, Ozil, and Durand were initially implemented, validated, and used to generate various results related to the performance of the active layer with changes in the thermodynamic conditions and geometry. The Agglomerate Model was then further developed, implemented, and validated to include among other things pores, flooding, and both humidified air and humidified O₂. All models were implemented and solved using FEM and a computational fluid dynamics (CFD) solver, developed by Blue Ridge Numeric Inc. (BRNI) called CFDesign. The use of these models for the discrete modeling of platinum particles is shown to be beneficial for understanding the behavior of a fuel cell. The addition of gas pores is shown to promote high current densities due to increased species transport throughout the agglomerate. Flooding is considered, and its effect on the cathode active layer is evaluated. The model takes various transport and electrochemical kinetic parameters values from the literature in order to do a parametric study

showing the degree to which temperature, pressure, and geometry are crucial to overall performance. This parametric study quantifies among a number of other things the degree to which lower porosities for thick active layers and higher porosities for thin active layers are advantageous to fuel Cell performance. Cathode active layer performance is shown not to be solely a function of catalyst surface area but discrete catalyst placement within the agglomerate.

Keith Promislow and Brian Wetton (2004), the authors develop a model of steady state thermal transfer in polymer electrolyte membrane fuel cell stacks. The model is appropriate for straight coolant channel unit cell designs and considers quantities averaged over the cross-channel direction, ignoring the impact of the gas and coolant channel geometries. At steady state and under the assumption that the membrane and electrodes are infinitesimally thin, a simple description can be made of the temperature distribution in the cells. The model provides estimates on two important quantities: the local temperature difference between coolant and membrane, and the spread of heat from an anomalously hot cell to its neighbour in a stack environment. The former question is easy to address after the model is presented. The latter requires small argument Laplace Transform asymptotics that corresponds to a large scaled heat transfer coefficient to the coolant channels. Results of computational approximation of the model are also shown and compared to the asymptotics.

McGarry and Grega (2005), the mass flow distribution and local flow structures that lead to areas of reactant starvation are explored for a small power large active area PEM fuel cell. A numerical model was created to examine the flow distribution for three different inlet profiles; blunt, partially developed, and fully developed. The different inlet profiles represent the various distances between the blower and the inlet to the fuel cell and the state of flow development. The partially and fully developed inlet profiles were found to have the largest percentage of cells that are deficient, 20% at a flow rate of 6.05 g/s. Three different inlet mass flow rates (stoichs) were also examined for each inlet profile. The largest percent of cells deficient in reactants is 27% and occurs at the highest flow rate of 9.1 g/s (3 stoichs) for the partially and fully developed turbulent profiles. In addition to the uneven flow distribution, flow separation occurs in the

front four channels for the blunt inlet profile at all flow rates examined. These areas of flow separation lead to localized reactant deficient areas within a channel.

Qingyun Liu and Junxiao Wu (2005), a multi-resolution simulation method was developed for the polymer electrolyte membrane (PEM) fuel cell simulation: a full 3D model was employed for the membrane and diffusion layer; a 1D+2D model was applied to the catalyst layer, that is, at each location of the fuel cell plate, the governing equations were integrated only in the direction perpendicular to the fuel cell plate; and a quasi-1D model with high numerical efficiency and reasonable accuracy was employed for the flow channels. The simulation accuracy was assessed in terms of the fuel cell polarization curves and membrane Ohmic over potential. Overall, good agreements between the simulated results and the experimental data were obtained. However, at large current densities, with high relative humidity reactant inputs, the simulation under-predicted the fuel cell performance due to the single-phase assumption; the simulation slightly over-predicted the fuel cell performance for a dry cathode input, possibly due to the non-linearity of the membrane properties in dehydration case. Further, a parameter study was performed under both fully humidified and relatively dry conditions for the parameters related to the cathode catalyst layer and the gas diffusion layer (GDL). It is found that the effects of liquid water in both the GDL and catalyst layer on the cell performance, and the accurate identification of the cathode catalyst layer parameters such as the cathodic transfer coefficient should be focused for future studies in order to further improve the model accuracy.

Shaoping Li, William Wangard and Ulrich Becker (2005), a 3-dimensional, two-phase Computational Fluid Dynamics (CFD) model for PEMFC simulations has been developed and implemented in FLUENT, a general-purpose commercial software package with multi-physics capabilities. The model formulation was given in details in the previous ASME fuel cell conference, together with in-situ distributions of current densities and species concentrations computed for a simple geometry. In this paper, numerical performance of this model in terms of computing time and parallel efficiency are assessed through the computation of a relatively larger-size fuel cell (50 cm^2) with serpentine channels. The convergence history and parallel performance data show that the Fluent's PEMFC model is

numerically robust and efficient. In addition to the numerical performance, the physical validity of the model is tested through comparisons with experimental data of polarization curves and local current density distributions from the most recent work of Mench. Comparisons with the data show good agreement in the overall polarization curves and reasonably good agreement in local current density distributions too. The comma-shaped local polarization curves seen in the experiments are qualitatively correctly captured. Moreover, our computations show that hydrogen mass fraction and molar concentration can both increase along the anode flow channel, despite that hydrogen is being depleted in the anodic electrochemical reaction. The reason for this to happen is that the osmotic drag moves the water from anode to cathode at a much faster rate than the hydrogen depletion rate. An analytical derivation that reveals the relationship between species molar concentration and mass fraction is also given.

Shih-Hung Chan and Karam Beshay (2005), the proton-exchange membrane (PEM) fuel cell works under low temperatures and hence is suitable for the automotive industry. The produced water vapor in the vicinity of the membrane may condense into liquid water, if the water mass fraction is higher than the saturation value corresponding to the local temperature. In this case the flowing fluid inside the layers of the PEMFC is a 2-phase flow. The locally homogeneous flow (LHF) model has been previously used for modeling the 2-phase flow in PEM fuel cells, with limited success. This model could not predict the blocking effect of the liquid phase, since both phases flow locally with the same velocity, according to the LHF model. In contrast to complete coupling of the two phases, assumed by the LHF model, a blocking model was used by some investigators where the liquid is totally uncoupled to the gas phase. This assumption causes the liquid to become essentially stationary inside the pores of the GDL and catalyst layers and hence only the gas phase equations need to be considered. Both of these extreme models were only successful to a limited extent. Numerical computations are carried out for a typical proton exchange membrane fuel cell that has experimental data. In order to obtain complete performance results, the computations are repeated for increasing fuel cell electric current densities until the limiting current is reached. The obtained two-fluid and single-phase simulations are compared with the corresponding experimental and numerical data

available in the literature. The 2-fluid model shows that the blocking effect of the liquid phase starts to dominate, for cell voltage less than 0.65 V; in this case, the flowing 2-phase flow produces faster drop in cell voltage as the loading electric current increases. This phenomenon was partially hindered by the LHF model but essentially completely bypassed by the single-phase simulations. The 2-fluid simulations show that most of the liquid dispersed phase is concentrated in the cathode, reaching maximum value near the cathode catalyst layer- membrane interface. This behavior results from the lack of mobility of the liquid water inside the pores.

CHAPTER 3

FUEL CELL

3.1 INTRODUCTION

A fuel cell is an electrochemical device, which directly converts chemical energy stored in a fuel and an oxidizer into electrical energy.

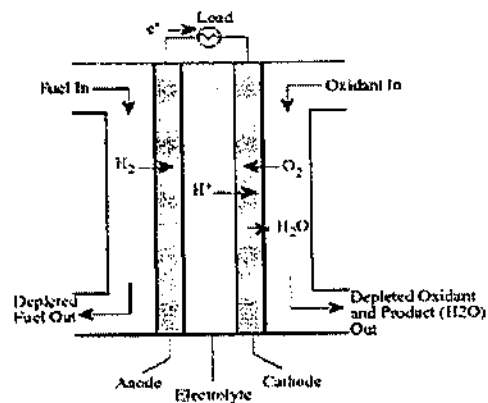


FIGURE 3.1 FUEL CELL

In principle, a fuel cell operates like a battery. Unlike a battery, a fuel cell does not run down or require recharging. It will produce energy in the form of electricity and heat as long as fuel is supplied.

A fuel cell consists of two electrodes sandwiched around an electrolyte as shown in Figure 3.1. Oxygen passes over one electrode and hydrogen over the other, generating electricity, water and heat.

Hydrogen fuel is fed into the "anode" of the fuel cell. Oxygen (or air) enters the fuel cell through the cathode. Encouraged by a catalyst, the hydrogen atom splits into a proton and an electron, which take different paths to the cathode. The proton passes through the electrolyte. The electrons create a separate current that can be utilized before they return to the cathode, to be reunited with the hydrogen and oxygen in a molecule of water.

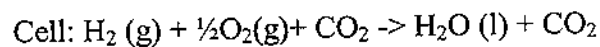
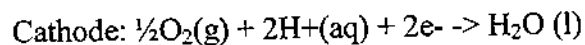
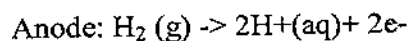
A fuel cell system, which includes a "fuel reformer", can utilize the hydrogen from any hydrocarbon fuel - from natural gas to methanol, and even gasoline. Since the fuel cell relies on chemistry and not combustion, emissions from this type of a system would still be much smaller than emissions from the cleanest fuel combustion processes.

3.2 TYPES OF FUEL CELL

3.2.1 Phosphoric Acid Fuel Cell (PAFC)

This type of fuel cell is commercially available today. More than 200 fuel cell systems have been installed all over the world - in hospitals, nursing homes, hotels, office buildings, schools, utility power plants, an airport terminal, landfills and waste water treatment plants. PAFC's generate electricity at more than 40% efficiency and nearly 85% of the steam this fuel cell produces is used for cogeneration, this compares to about 35% for the utility power grid in the United States.

Operating temperatures are in the range of 300 to 400°F (150 – 200°C). At lower temperatures, phosphoric acid is a poor ionic conductor, and carbon monoxide (CO) poisoning of the Platinum (Pt) electro-catalyst in the anode becomes severe. The electrolyte is liquid phosphoric acid soaked in a matrix. One of the main advantages to this type of fuel cell, besides the nearly 85% cogeneration efficiency, is that it can use impure hydrogen as fuel. PAFCs can tolerate a CO concentration of about 1.5 percent, which broadens the choice of fuels they can use. If gasoline is used, the sulfur must be removed. Disadvantages of PAFC's include: it uses expensive platinum as a catalyst, it generates low current and power comparably to other types of fuel cells, and it generally has a large size and weight. PAFC's, however, are the most mature fuel cell technology. Through organizational linkages with Gas Research Institute (GRI), electronic utilities, energy service companies, and user groups, the Department of Energy (DOE) helped in bringing about the commercialization of a PAFC, produced by ONSI (now **UTC Fuel Cells**). Existing PAFC's have outputs up to 200 kW, and 1 MW units have been tested.



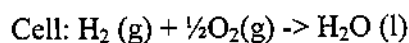
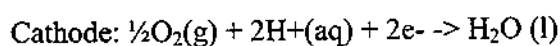
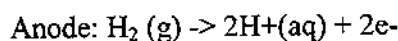
3.2.2 Polymer Electrolyte Membrane (PEM)

These cells operate at relatively low temperatures (about 175°F or 80°C), have high power density, can vary their output quickly to meet shifts in power demand, and are suited for applications, such as in automobiles; where quick startup is required. According to DOE, "They are the primary candidates for light-duty vehicles, for

buildings, and potentially for much smaller applications such as replacements for rechargeable batteries".

The Polymer Electrolyte Membrane is a thin plastic sheet that allows hydrogen ions to pass through it. The membrane is coated on both sides with highly dispersed metal alloy particles (mostly platinum) that are active catalysts. The electrolyte used is a solid organic polymer poly-perflourosulfonic acid. The solid electrolyte is an advantage because it reduces corrosion and management problems. Hydrogen is fed to the anode side of the fuel cell where the catalyst encourages the hydrogen atoms to release electrons and become hydrogen ions (protons).

The electrons travel in the form of an electric current that can be utilized before it returns to the cathode side of the fuel cell where oxygen has been fed. At the same time, the protons diffuse through the membrane (electrolyte) to the cathode, where the hydrogen atom is recombined and reacted with oxygen to produce water, thus completing the overall process. This type of fuel cell is, however, sensitive to fuel impurities. Cell outputs generally range from 50 to 250 kW.



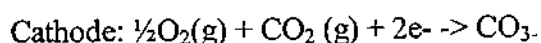
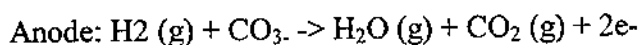
3.2.3 Molten Carbonate Fuel Cell (MCFC)

These fuel cells use a liquid solution of lithium, sodium and/or potassium carbonates, soaked in a matrix for an electrolyte. They promise high fuel-to-electricity efficiencies, about 60% normally or 85% with cogeneration, and operate at about 1,200⁰F or 650⁰C.

The high operating temperature is needed to achieve sufficient conductivity of the electrolyte. Because of this high temperature, noble metal catalysts are not required for the cell's electrochemical oxidation and reduction processes. To date, MCFC's have been operated on hydrogen, carbon monoxide, natural gas, propane, landfill gas, marine diesel, and simulated coal gasification products. 10 kW to 2 MW MCFC's have been tested on a variety of fuels and are primarily targeted to electric utility applications.

Carbonate fuel cells for stationary applications have been successfully demonstrated in Japan and Italy. The high operating temperature serves as a big advantage because this implies higher efficiency and the flexibility to use more

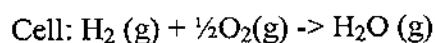
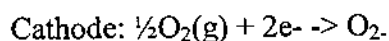
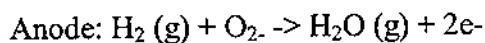
types of fuels and inexpensive catalysts as the reactions involving breaking of carbon bonds in larger hydrocarbon fuels occur much faster as the temperature is increased. A disadvantage to this, however, is that high temperatures enhance corrosion and the breakdown of cell components.



3.2.4 Solid Oxide Fuel Cell (SOFC)

Another highly promising fuel cell, this type could be used in big, high-power applications including industrial and large-scale central electricity generating stations. Some developers also see SOFC use in motor vehicles and are developing fuel cell auxiliary power units (APU) with SOFC's. A solid oxide system usually uses a hard ceramic material of solid zirconium oxide and a small amount of yttria, instead of a liquid electrolyte, allowing operating temperatures to reach 1,800⁰F or 1000⁰C.

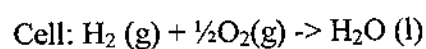
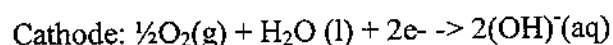
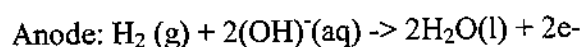
Power generating efficiencies could reach 60% and 85% with cogeneration and cell output is up to 100 kW. One type of SOFC uses an array of meter-long tubes, and other variations include a compressed disc that resembles the top of a soup can. Tubular SOFC designs are closer to commercialization and are being produced by several companies around the world. Demonstrations of tubular SOFC technology have produced as much as 220 kW. Japan has two 25 kW units online and a 100 kW plant being testing in Europe.



3.2.5 Alkaline

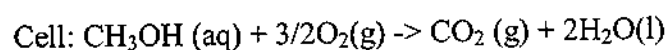
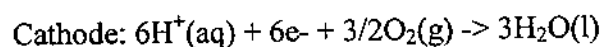
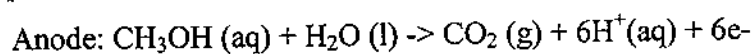
Long used by NASA on space missions, these cells can achieve power generating efficiencies of up to 70 percent. They were used on the Apollo spacecraft to provide both electricity and drinking water. Their operating temperature is 150 to 200⁰C (about 300 to 400⁰F). They use an aqueous solution of alkaline potassium hydroxide soaked in a matrix as the electrolyte. This is

advantageous because the cathode reaction is faster in the alkaline electrolyte, which means higher performance. Until recently they were too costly for commercial applications, but several companies are examining ways to reduce costs and improve operating flexibility. They typically have a cell output from 300 watts to 5 kW.



3.2.6 Direct Methanol Fuel Cell (DMFC)

These cells are similar to the PEM cells in that they both use a polymer membrane as the electrolyte. However, in the DMFC, the anode catalyst itself draws the hydrogen from the liquid methanol, eliminating the need for a fuel reformer. Efficiencies of about 40% are expected with this type of fuel cell, which would typically operate at a temperature between 120-190⁰F or 50 –100⁰C. This is a relatively low range, making this fuel cell attractive for tiny to mid-sized applications, to power cellular phones and laptops. Higher efficiencies are achieved at higher temperatures. A major problem, however, is fuel crossing over from the anode to the cathode without producing electricity. Many companies have said they solved this problem, however. They are working on DMFC prototypes used by the military for powering electronic equipment in the field.



3.2.7 Regenerative Fuel Cell

Regenerative fuel cells would be attractive as a closed-loop form of power generation. Water is separated into hydrogen and oxygen by a solar-powered electrolyser. The hydrogen and oxygen are fed into the fuel cell, which generates electricity, heat and water. The water is then re circulated back to the solar-powered electrolyser and the process begins again. NASA and others are currently researching these types of fuel cells worldwide.

3.2.8 Zinc-Air Fuel Cell (ZAFC)

In a typical zinc/air fuel cell, there is a gas diffusion electrode (GDE), a zinc anode separated by electrolyte, and some form of mechanical separators. The GDE is a permeable membrane that allows atmospheric oxygen to pass through. After the oxygen has converted into hydroxyl ions and water, the hydroxyl ions will travel through an electrolyte, and reaches the zinc anode. Here, it reacts with the zinc, and forms zinc oxide. This process creates an electrical potential; when a set of ZAFC cells are connected, the combined electrical potential of these cells can be used as a source of electric power. This electrochemical process is very similar to that of a PEM fuel cell, but the refueling is very different and shares characteristics with batteries.

ZAFC's contain a zinc "fuel tank" and a zinc refrigerator that automatically and silently regenerates the fuel. In this closed-loop system, electricity is created as zinc and oxygen are mixed in the presence of an electrolyte (like a PEMFC), creating zinc oxide. Once fuel is used up, the system is connected to the grid and the process is reversed, leaving once again pure zinc fuel pellets. The key is that this reversing process takes only about 5 minutes to complete, so the battery recharging time hang up is not an issue. The chief advantage zinc-air technology has over other battery technologies is its high specific energy, which is a key factor that determines the running duration of a battery relative to its weight. When ZAFC's are used to power EVs, they have proven to deliver longer driving distances between refuels than any other EV batteries of similar weight. Moreover, due to the abundance of zinc on earth, the material costs for ZAFC's and zinc-air batteries are low. Hence, zinc-air technology has a potential wide range of applications, ranging from EVs, consumer electronics to military. **Powerzinc** in southern California is currently commercializing their zinc/air technology for a number of different applications.

3.2.9 Protonic Ceramic Fuel Cell (PCFC)

This new type of fuel cell is based on a ceramic electrolyte material that exhibits high Protonic conductivity at elevated temperatures. PCFC's share the thermal and kinetic advantages of high temperature operation at 700⁰C with molten carbonate and solid oxide fuel cells, while exhibiting all of the intrinsic

benefits of proton conduction in polymer electrolyte and phosphoric acid fuel cells (PAFCs). The high operating temperature is necessary to achieve very high electrical fuel efficiency with hydrocarbon fuels.

PCFC's can operate at high temperatures and electrochemically oxidize fossil fuels directly to the anode. This eliminates the intermediate step of producing hydrogen through the costly reforming process. Gaseous molecules of the hydrocarbon fuel are absorbed on the surface of the anode in the presence of water vapor, and hydrogen atoms are efficiently stripped off to be absorbed into the electrolyte, with carbon dioxide as the primary reaction product. Additionally, PCFC's have a solid electrolyte so the membrane cannot dry out as with PEM fuel cells, or liquid can't leak out as with PAFCs. **CoorsTek** is primarily researching this type of fuel cell.

CHAPTER 4

COMPUTATIONAL FLUID DYNAMICS

4.1 INTRODUCTION

Computational Fluid Dynamics or simply CFD is concerned with obtaining numerical solution to fluid flow problems by using computers. The advent of high-speed and large-memory computers has enabled CFD to obtain solutions to many flow problems including those that are compressible or incompressible, laminar or turbulent, chemically reacting or non-reacting.

The equations governing the fluid flow problem are the continuity (conservation of mass), the Navier-Stokes (conservation of momentum), and the energy equations. These equations form a system of coupled non-linear partial differential equations (PDE's). Because of the non-linear terms in these PDE's, analytical methods can yield very few solutions. In general, closed form analytical solutions are possible only if these PDE's can be made linear, either because non-linear terms naturally drop out (e.g., fully developed flows in ducts and flows that are in viscose and irrotational everywhere) or because nonlinear terms are small compared to other terms so that they can be neglected (e.g., creeping flows, small amplitude sloshing of liquid etc.). If the non-linearity in the governing PDE's cannot be neglected, which is the situation for most engineering flows, then numerical methods are needed to obtain solutions.

CFD is the art of replacing the differential equation governing the Fluid Flow, with a set of algebraic equations (the process is called Discretisation), that in turn can be solved with the aid of a digital computer to get an approximate solution. The well-known Discretisation methods used in CFD are Finite Difference Method (FDM), Finite Volume Method (FVM), Finite Element Method (FEM), and Boundary Element Method (BEM).

FDM is the most commonly used method in CFD applications. Here the domain including the boundary of the physical problem is covered by a grid or mesh. At each of the interior grid point the original Differential Equations are replaced by equivalent finite difference approximations. In making this replacement, we introduce an error, which is proportional to the size of the grid. Making the grid size smaller to get an accurate solution within some specified tolerance can reduce this error.

Commercial CFD codes such as FLUENT, PHOENIX, CFX, CFD++ and Star-CD have also developed to a point that the user need not be an expert on CFD in order to successfully put it to use. The end-user must however have a good knowledge of fluid dynamics for a successful simulation with credible results to be obtained. Therefore, used correctly, CFD codes can reduce time and cost of experiments in product development or process improvement.

The rest of the chapter discusses the various areas of CFD in the following order:

- Governing equations
- Grid generation techniques
- Boundary conditions that define a CFD problem
- Solution algorithms and convergence criteria
- Basic background on the CFD solver used (FLUENT)

4.2 GOVERNING EQUATIONS

The governing equations of fluid behavior are given in equations. These equations are given for compressible flow, but can be easily simplified for incompressible flow. In the Eulerian system, the particle derivative is described as follows

$$\frac{D}{Dt} = \frac{\partial}{\partial t} + (\bar{V} \cdot \nabla) \quad \text{---- (4.1)}$$

Where

$$(\bar{V} \cdot \nabla) = d\bar{V} = \frac{\partial u}{\partial x} + \frac{\partial v}{\partial y} + \frac{\partial w}{\partial z} \quad \text{---- (4.2)}$$

This particle derivative will be used in the sections to follow to present the Navier-Stokes equations in conservative form.

4.2.1 Conservation of Mass

The equation for conservation of mass in conservative form is given as

$$\frac{\partial \rho}{\partial t} + \nabla \cdot (\rho \bar{V}) \quad \text{---- (4.3)}$$

Where ρ is the density and \bar{V} is the vector velocity of the fluid.

4.2.2 Conservation of Momentum

The equations for conservation of momentum in the three Cartesian directions are presented.

$$\begin{aligned} & \frac{\partial(\rho u)}{\partial t} + \frac{\partial(\rho u^2)}{\partial x} + \frac{\partial(\rho uv)}{\partial y} + \frac{\partial(\rho uw)}{\partial z} \\ &= \frac{\partial p}{\partial x} + \frac{\partial}{\partial x} \left(\lambda \nabla \bar{V} + 2\mu \frac{\partial u}{\partial x} \right) + \frac{\partial}{\partial y} \left[\mu \left(\frac{\partial v}{\partial x} + \frac{\partial u}{\partial y} \right) \right] + \frac{\partial}{\partial z} \left[\mu \left(\frac{\partial u}{\partial z} + \frac{\partial w}{\partial x} \right) \right] + \rho g_x \end{aligned}$$

---- (4.4)

$$\begin{aligned} & \frac{\partial(\rho v)}{\partial t} + \frac{\partial(\rho uv)}{\partial x} + \frac{\partial(\rho v^2)}{\partial y} + \frac{\partial(\rho vw)}{\partial z} \\ &= -\frac{\partial p}{\partial y} + \frac{\partial}{\partial y} \left(\lambda \nabla \bar{V} + 2\mu \frac{\partial v}{\partial y} \right) + \frac{\partial}{\partial x} \left[\mu \left(\frac{\partial v}{\partial x} + \frac{\partial u}{\partial y} \right) \right] + \frac{\partial}{\partial z} \left[\mu \left(\frac{\partial w}{\partial y} + \frac{\partial v}{\partial z} \right) \right] + \rho g_y \end{aligned}$$

---- (4.5)

$$\begin{aligned} & \frac{\partial(\rho w)}{\partial t} + \frac{\partial(\rho uw)}{\partial x} + \frac{\partial(\rho vw)}{\partial y} + \frac{\partial(\rho w^2)}{\partial z} \\ &= -\frac{\partial p}{\partial z} + \frac{\partial}{\partial x} \left[\mu \left(\frac{\partial u}{\partial z} + \frac{\partial w}{\partial x} \right) \right] + \frac{\partial}{\partial y} \left[\mu \left(\frac{\partial w}{\partial x} + \frac{\partial v}{\partial z} \right) \right] + \frac{\partial}{\partial z} \left[\lambda \nabla \bar{V} + 2\mu \frac{\partial w}{\partial z} \right] + \rho g_z \end{aligned}$$

---- (4.6)

These equations can be rewritten as a single vector equation using indicial notation:

$$\frac{D\rho\bar{V}}{Dt} = \rho \bar{g} - \Delta p + \frac{\partial}{\partial x_j} \left[\mu \left(\frac{\partial v}{\partial x_j} + \frac{\partial v_j}{\partial x_i} \right) + \delta_{ij} \lambda d\bar{V} \right] \quad \text{---- (4.7)}$$

4.2.3 The Energy Equation

The energy equation, which in essence is the first law of thermodynamics, is given in its most economic form as follows:

$$\rho \frac{D}{Dt} \left[e + \frac{p}{\rho} \right] - \frac{Dp}{Dt} + d(K \nabla T) + \tau_{ij} \frac{\partial u_i}{\partial x_j} \quad \text{---- (4.8)}$$

Where the viscous stresses are given by the stress tensor:

$$\tau_{ij} = \mu \left(\frac{\partial u_i}{\partial x_j} + \frac{\partial u_j}{\partial x_i} \right) \quad \text{---- (4.9)}$$

4.3 PROGRAM STRUCTURE

Figure 4.1 shows the organizational structure of these components.

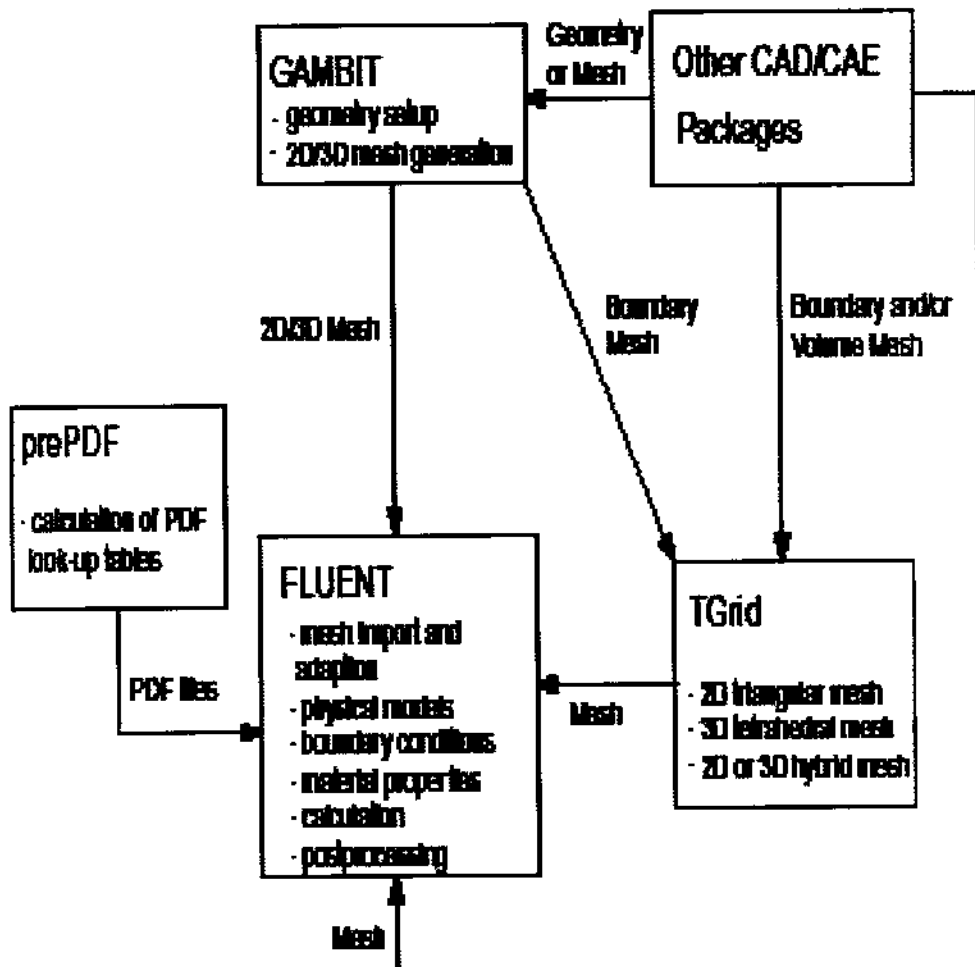


FIGURE 4.1 BASIC PROGRAM STRUCTURE

FLUENT package includes the following products:

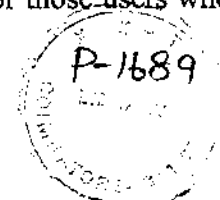
- FLUENT - the solver.
- PrePDF - the preprocessor for modeling non-premixed combustion in FLUENT.
- GAMBIT - the preprocessor for geometry modeling and mesh generation.
- Tgrid - an additional preprocessor that can generate volume meshes from existing Boundary meshes.
- Translators - (translators) for import of surface and volume meshes from CAD/CAE packages such as ANSYS, CGNS, I-DEAS, NASTRAN, PATRAN, and others.

GAMBIT is used to create geometry and grid. See the GAMBIT documentation for details. Also use TGrid to generate a triangular, tetrahedral, or hybrid volume Mesh from an existing boundary mesh (created by GAMBIT or a third-party CAD/CAE Package). See the TGrid User's Guide for details. It is also possible to create grids for FLUENT using ANSYS (Swanson Analysis Systems, Inc.), CGNS (CFD general notation System), or I-DEAS (SDRC); or MSC/ARIES, MSC/PATRAN, or MSC/NASTRAN (all from MacNeal-Schwendler Corporation). Interfaces to other CAD/CAE packages may be made Available in the future, based on customer requirements, but most CAD/CAE packages can export grids in one of the above formats.

Once a grid has been read into FLUENT, all remaining operations are performed within the solver. These include setting boundary conditions, defining fluid properties, executing the solution, refining the grid, and viewing and post processing the results. Note that preBFC and GeoMesh are the names of Fluent preprocessors that were used before the introduction of GAMBIT. You may see some references to preBFC and GeoMesh in this manual, for those users who are still using grids created by these programs.

4.3.1 Grid generation and GAMBIT

The grid generation process or meshing involves dividing the flow domain into smaller control volumes over which the discretised Navier-Stokes equations



are solved. Grid (mesh) types can be classified into two categories namely; structured and unstructured grids. The mentioned types of grids find use in different applications and used in the meshing process in this study.

Structured grids consist of grid lines with a characteristic of not crossing or overlapping. The position of any grid point is uniquely identified by a set of two (2-D) or three (3-D) dimensional indices, e.g., (i, j, k) . Unstructured grids make no assumption about any structure in the grid definition and usually consist of triangular (tetrahedral (tet) in 3D) elements.

A numerically generated structured grid or mesh, is understood here to be the organized set of points formed by the intersections of the lines of a boundary conforming to a curvilinear coordinate system. The prime feature of such a system is that some coordinate line (surface in 3D) is coincident with each segment of the boundary of the physical region.

The use of coordinate line intersections to define the grid points provides an organizational structure that allows all computations to be done on a fixed square grid when partial differential equations of interest have been transformed so that the curvilinear coordinates replace the Cartesian coordinates as the independent variables. This grid frees the computational simulation from restriction to certain boundary shapes and allows general flow solvers to be written in which the boundary shape is specified simply by input.

Grid generation for the purposes of this research takes place in FLUENT's pre-processor, GAMBIT. GAMBIT is a versatile pre-processor that can support a large variety of commercially available computer-aided design (CAD) platforms. Raw geometry can be imported from these CAD packages into GAMBIT where it is operated on (i.e., the necessary simplification for CFD purposes are made), in preparation for meshing.

Various meshing schemes are available in GAMBIT and are used where suitable in the grid generation process. Most of these schemes are unique to GAMBIT and are not necessarily documented, as they may be modifications of existing meshing schemes. GAMBIT allows the user to specify any volume to be meshed, although the shape and topological characteristics of the volume determine which mesh schemes can be used.

Different meshing schemes such as Hex, Hex/wedge and Tet Hybrid, can be specified on volumes to be meshed. The Hex mesh is composed of hexahedral

elements only constituting a fully structured mesh. The Hex/wedge mesh comprises mainly of hexahedral elements with wedge elements where necessary. However, Hex and Hex/wedge elements do not apply to any shape volume, as opposed to Tet Hybrid meshes. The versatility of the Tet Hybrid element makes it appreciable for use where the volume is complex and none of the other meshes can be applied. Solution inaccuracies associated with the Tet Hybrid element type are, however, more significant than for any of the other element types. Each element type is associated with a volume-meshing scheme and only those schemes used in this study will be discussed.

4.3.2 Boundary Conditions

In mathematics, any solution to a set of partial differential equations (PDE's) requires a set of boundary conditions for closure and the solution of the governing equations is no exception.

CFD simulations largely depend on the boundary conditions specified; hence correct boundary specification improves convergence to a correct solution. Incorrect boundary and initial conditions, however, can give convergence although not to a correct solution. There are wide variety of boundary types available in FLUENT, but only those used in this study will be given.

Flow inlet and exit boundaries

Pressure inlet: Used to define the total pressure and other scalar quantities at flow inlets.

Pressure outlet: Used to define the static pressure at flow outlets (and also other scalar variables, in case of backflow). The use of a pressure outlet boundary condition instead of an outflow condition often results in a better rate of convergence when backflow occurs during iteration. Note that when backflow occurs, this boundary acts like a pressure inlet boundary.

Wall and symmetry:

Wall: Used to define a solid-fluid interface where viscous flow is considered, thus applying a no-slip condition. The boundary condition on a surface assumes no relative velocity between the surface and the gas immediately at the surface.

Symmetry: Used to define surfaces at which normal velocity and normal gradients of all other variables are zero. This boundary type is essential where the geometry is symmetrical in nature, and only half the domain is specified.

4.3.3 Solution Algorithms

The governing equations of fluid flow are particularly difficult to solve because of their non-linear nature. Much work has been done in numerical methods to solve for these types of equations. Some proven and popular methods worthy of note are SIMPLE, SIMPLE-C, SIMPLER, QUICK and PISO. These methods are appreciated because of their robustness when applied to a variety of problems. In this study, steady state and transient flows are solved using the SIMPLE and PISO algorithms respectively.

The acronym, SIMPLE, stands for Semi-Implicit Method of Pressure-Linked Equations, and describes the iterative procedure by which a solution to discretised equations is obtained. This method is well suited to steady-state solution computation. The iterative procedure is the pseudo-transient treatment of the unsteady governing equations in a discrete form to obtain a steady-state solution. Patankar and Spalding introduced SIMPLE. The SIMPLE algorithm has a limitation in that new velocities and corresponding fluxes do not satisfy the momentum balance after the pressure-correction equation is solved. As a result, the calculation must be repeated until the balance is satisfied. The PISO algorithm improves the efficiency of this calculation by performing two additional corrections namely, neighbour and skewness correction.

PISO, which stands for Pressure-Implicit with Splitting of Operators, is a pressure-velocity coupling scheme that is part of the SIMPLE family of algorithms. This scheme is based on the higher degree of the approximate relation between the corrections for pressure and velocity. In highly distorted meshes, the approximate relationship between the correction of mass flux at the cell face and the difference of the pressure corrections at the adjacent cells is very rough. An iterative process is required to solve for the pressure-correction gradient components along cell faces since they are not known beforehand leading to the introduction of a process named skewness correction. Here, the pressure-

correction gradient is recalculated and used to update the mass flux corrections after the initial solution of the pressure-correction equation is obtained. This process significantly reduces convergence difficulties associated with highly distorted meshes and allows FLUENT to obtain solution on a highly skewed mesh in approximately the same number of iterations as required for a more orthogonal mesh. The PISO algorithm is used in this study for calculation of the unsteady gas behavior due to its efficient nature and suitability for transient computations as recommended in FLUENT.

4.3.4 Convergences

Convergence of a flow or heat problem can be judged by observing the normalized residuals. Residuals are numerical imbalances from the solved governing equations resulting from an incomplete solution during the iterative process. The solution process can be terminated when the normalized residuals fall below a specified value, which is generally 10^{-3} . However, in some cases even with the convergence criteria (as far as normalized residuals are concerned) satisfied, the solution may not necessarily be a correct one. To avoid such instances, quantities such as mass flow rate; static pressure and heat flux can be monitored at a location in the flow domain that is deemed to be important. The monitored quantity is observed until the change from iteration to iteration is negligible thus ensuring good convergence.

4.3.5 Background on the CFD solver used (FLUENT)

FLUENT is a finite volume (FV) solver that can handle a wide variety of flow problems such as external flow, internal flow, and two-phase flow. All modes of heat transfer can also be solved by the CFD code. This code is used for all CFD analyses throughout this study.

Modern CFD packages are user-friendly with improved user and code interfacing. Thus understanding the underlying principles of flow is important in order to put the code to good use. FLUENT has a facility for coding to make repetitive simulations, as in an optimization loop, more efficient and hence save time. This facility makes use of a journal file, which is a file containing a list of

- Definition of fluid properties.
- Specification of appropriate boundary conditions at cells, which coincide with or touch the domain boundary.

4.4.2 Solver

The numerical methods that form the basis of the solver perform the following steps:

- Approximation of the unknown flow variables by means of simple functions.
- Discretisation by substitution of the approximations into the governing flow equations and subsequent mathematical manipulations.
- Solution of the algebraic equations.

4.4.3 Post-processor

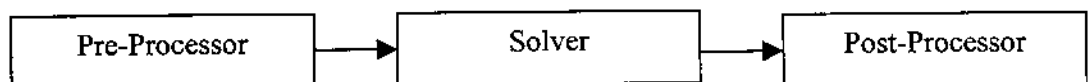
CFD packages are now equipped with versatile data visualization tools.

These include

- Domain geometry & Grid display.
- Vector plot.
- Line and shaded contour plot.
- 2D & 3D surface plots.
- Particle tracking.
- View manipulation (Translation, Rotational, Scaling).
- Color postscript output.

4.4.4 CFD Simulation

The process of performing single CFD simulation is split into components.



Setting up the simulation	: Pre-processor
Solving for the Flow Field	: Solver
Visualizing the Results	: Post-processor

4.5 PROBLEM SOLVING STEPS

Once you have determined the important features of the problem you want to solve, you will follow the basic procedural steps shown below.

1. Creating the model geometry and grid.
2. Starting the appropriate solver for 2D or 3D modeling.
3. Importing the grid.
4. Checking the grid.
5. Selecting the solver formulation.
6. Choosing the basic equations to be solved: laminar or turbulent (or in viscid), chemical Species or reaction, heat transfer models, etc. Identify additional models needed: Fans, heat exchangers, porous media, etc.
7. Specifying material properties.
8. Specifying the boundary conditions.
9. Adjusting the solution control parameters.
10. Initializing the flow field.
11. Calculating a solution.
12. Examining the results.
13. Saving the results.

CHAPTER 5

MODEL DEVELOPMENT

phenomenon. In brief, the model uses a one-dimensional approach where the independent variables are the electrical potential of the solid (ϕ_s) and liquid (ϕ_l) phases, the hydraulic pressure (P), concentration of Hydrogen (C_{H_2}) and oxygen (C_{O_2}) in the liquid phase.

The Figure 5.2 shows the cell configuration for the CFD model of the PEM Fuel Cell.

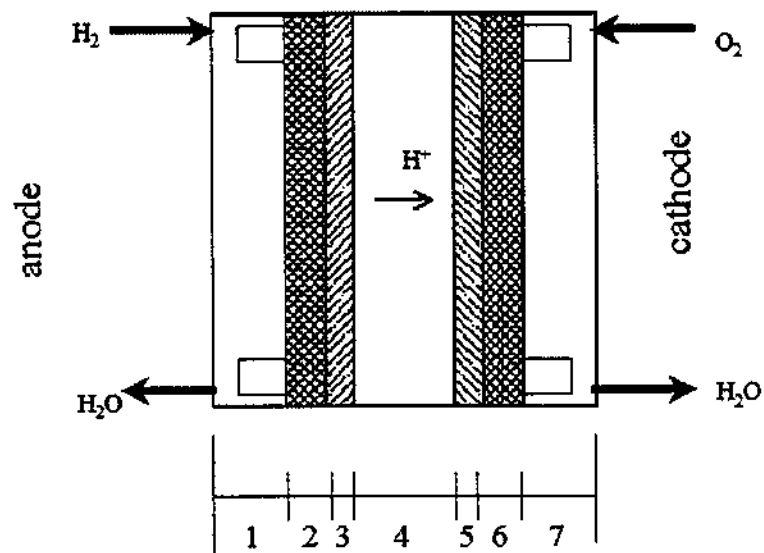


FIGURE 5.2 CELL CONFIGURATION FOR THE CFD MODEL

The Regions in the Figure 5.2 are:

- 1-Anode Flow Channel
- 2-Anode Diffusion Layer
- 3-Anode Catalyst Layer
- 4-Polymer Electrolyte Membrane
- 5-Cathode Catalyst Layer
- 6-Cathode Diffusion Layer
- 7-Cathode Flow Channel

5.3 MODEL DESCRIPTION AND FIELD EQUATIONS

The model presented here is a full three-dimensional model that resolves coupled transport processes in the membrane, catalyst layer, gas diffusion electrodes and reactant flow channels of a PEM fuel cell. The model was implemented via a set of user-defined subroutines in a commercial CFD code, Fluent 6.1. The implementation allows simulations using parallel processing. The assumptions and governing equations are presented in this section.

5.3.1 Assumptions

Under constant load conditions, a fuel cell is assumed to operate in steady state. Since the gas streams in the flow channels are humidified, hydrogen and air at low velocities, laminar flow and ideal gas behavior are assumed. The complex nature of the transport processes in PEM fuel cells precludes systematic modeling of all processes in a three-dimensional model, and phenomena that are second order under normal operating conditions are neglected:

- Steady-state operation of the cell.
- Constant temperature (isothermal) operation of the cell.
- Zero differential gas pressure in the porous medium.
- Liquid-phase transport at the anode.
- All water produced in the electrochemical reactions is assumed to be in the gas phase, and phase change and phase-transport are not considered.
- The membrane is assumed to be fully humidified and its Protonic conductivity is taken to be constant.
- The membrane is considered impermeable to gases and crossover of reactant gases is neglected.
- Ohmic heating in the bipolar plates and in the gas diffusion electrodes is neglected due to high conductivity.

5.3.2 Model equations in gas flow channel

CFD codes are structured around numerical algorithms that solve equations representing physical conservation laws (mass conservation, momentum conservation species conservation) in order to obtain the velocity field and associated mass, heat and scalar transport quantities.

The one-dimensional steady state mass conservation equation is given by:

$$\frac{\partial}{\partial x}(\epsilon \rho u) = 0 \quad \text{---- (5.1)}$$

The momentum conservation equation is given by:

$$\frac{\partial}{\partial x}(\epsilon \rho u^2) + \frac{\partial}{\partial x}(P) = -\frac{\mu}{K_p}(\epsilon^2 u) \quad \text{---- (5.2)}$$

The species conservation equation is given by:

$$\frac{\partial}{\partial x}(\epsilon \rho u C^k) - \frac{\partial}{\partial x}\left(D_k \frac{\partial}{\partial x}\{C^k\}\right) = 0 \quad \text{---- (5.3)}$$

Charge Conservation equation is given by:

$$\frac{\partial}{\partial x}\left(\sigma_e \frac{\partial}{\partial x}\{\phi_s\}\right) = 0 \quad \text{---- (5.4)}$$

The density of the mixture is calculated using:

$$\rho = \frac{1}{\sum_i \frac{y_i}{\rho_i}} \quad \text{---- (5.5)}$$

Density of each species is obtained from the perfect gas law relation:

$$\rho_i = \frac{p_{op} M_i}{RT} \quad \text{---- (5.6)}$$

In which p_{op} corresponds to the anode or cathode side pressure, M_i is the molecular weight, T is the temperature and R is the universal gas constant.

5.3.4 Energy transport

The energy equation, which expresses the first law of thermodynamics, can be expressed as:

$$\nabla \cdot (\rho \mathbf{E} + p) = \nabla \cdot \left(k_{eff} \nabla T - \sum_j h_j \mathbf{j}_j + (\tau_{eff,v}) \right) + S_h \quad \text{---- (5.10)}$$

Where E is the total energy, k_{eff} is the effective conductivity, and \mathbf{j}_j is the diffusion flux of species j and h is the enthalpy, τ_{eff} is the effective stress tensor matrix and S_h is the source term per unit volume per unit time. However, the dissipation energy will be very low in the fuel cell due to low velocity laminar flow and can be omitted from the energy equation. The first three terms on the right-hand side of equation represent the energy transfer due to conduction, species diffusion, and viscous dissipation, respectively.

5.3.5 Model equations in gas diffusion layer

The gas diffusion electrodes consist of carbon cloth or carbon fiber paper and can be considered as porous media through which reactant gases are distributed to the catalyst layer, while the solid matrix of the layer collects current and connects the reaction zone to the collector plates. The equations that govern gas transport phenomena in the diffusion layers are similar to those used in the channels with the addition of a porosity parameter. The mass conservation equation is expressed as:

$$\nabla \cdot (\rho \mathbf{v}) = S_m \quad \text{---- (5.11)}$$

In which S_m is a mass source, specified for the anode and cathode.

In Fluent 6.1, a superficial velocity, based on the volumetric flow rate, is used inside the porous medium. This superficial velocity is also used to ensure continuity of the velocity vectors across the porous medium interface. More accurate simulations of porous media flows would require solution of the physical velocity throughout the flow-field, rather than the superficial velocity. Fluent 6.1 provides the possibility of solving the transport equation in the porous media

using the physical velocity. However, the inlet mass flow is calculated from the superficial velocity and therefore the pressure drop across the porous media would be the same whether the physical or superficial velocity formulation is used.

The porous media model essentially consists of an extra momentum sink term added to the standard fluid flow. This source term consist of two loss terms, viscous and inertial:

$$S_{mom,i} = - \left(\sum_{j=1}^3 D_{ij} \mu v_j + \sum_{j=1}^3 C_{ij} \frac{1}{2} \rho v_j \right) \quad \text{---- (5.12)}$$

Where $S_{mom,i}$ is the source term for the momentum equation in the x, C is the inertial resistance factor matrix and D is a matrix containing the inverse of the permeability. Note that the inertial loss term is only significant for high flow velocities, and its contribution is negligible in the present model. The momentum sink generates a pressure gradient in the porous region.

5.3.6 Mass transport equation in porous media

The steady state species transport equation in porous media takes the form:

$$\nabla \cdot (\rho \gamma y_i) = \nabla \cdot \left(\rho \gamma D_i^{eff} \nabla y_i \right) + S_i \quad \text{---- (5.13)}$$

Is an effective diffusion coefficient that takes into account the effect of additional drag by the irregular shape and the actual length of the pores in comparison with a bundle of straight parallel capillaries with constant diameter, and is given by:

$$D_i^{eff} = \gamma \frac{D_i}{\mu_p} \quad \text{---- (5.14)}$$

Where D_i is the diffusion coefficient.

5.3.7 Energy transport in porous media

Equation is used to calculate the energy transport in the porous media with an effective thermal conductivity, k_{eff} , calculated as the volume average of the fluid conductivity and the solid conductivity (assuming thermodynamic equilibrium), i.e.:

$$K_{eff} = \gamma k_f + (1 - \gamma) k_s \quad \text{---- (5.15)}$$

Where k_f is the thermal conductivity in the fluid phase and k_s is the solid medium thermal conductivity.

5.3.8 Potential

The potential distribution in the gas diffusion layer can be calculated by applying the generic transport equation without the convective terms.

$$-\nabla \cdot (\sigma \nabla \phi) = S_\phi \quad \text{---- (5.16)}$$

Where s is the electronic conductivity.

5.3.9 Catalyst layer

Current calculations

The current density at both cathode and anode is calculated using equation:

$$i = i^+ + i^- = i_o \left[\exp\left(\frac{\beta n F \eta}{RT}\right) - \exp\left(-\frac{(1 - \beta) n F \eta}{RT}\right) \right] \quad \text{---- (5.17)}$$

Where i_o is the exchange current density, n is the number of electrons per mole of reactant and R is the universal gas constant, β is the asymmetry parameter, which is determined empirically to be between 0.4 and 0.6. The sensitivity of the model to this parameter will be discussed subsequently.

5.3.10 Boundary conditions

Boundary conditions are required at all boundaries of the computational domains, as well as at internal interfaces.

Inlet

At the inlet of both anode and cathode flow channels the boundary values are prescribed from the stoichiometric flow rate, temperature and mass fractions.

The mass flow rate at the inlet is prescribed in conjunction with a fully developed laminar flow profile. Exact solutions for such profiles are available for a variety of cross-sectional areas, but we found it computationally more effective to use an approximation, which provides values within 1% of the exact solution:

$$u = u_{\max} \left(1 - \left(\frac{y}{b} \right)^n \right) \left(1 - \left(\frac{z}{a} \right)^m \right) \quad \text{---- (5.18 A)}$$

$$u_{\max} = u_m \left(\frac{m+1}{m} \right) \left(\frac{n+1}{n} \right) \quad \text{---- (5.18 B)}$$

Where u_{\max} is the maximum velocity, a is the half-width of a non-circular duct, b is the half-height of a non-circular duct and u_m is the average velocity. Relations for the values m and n are:

$$m = 1.7 + 0.5 \left(\frac{a}{b} \right)^{-1.4} \quad \text{---- (5.19 A)}$$

$$n = \begin{cases} 2, & \text{for } \frac{a}{b} \leq \frac{1}{3} \\ 2 + 0.3 \left(\frac{a}{b} - \frac{1}{3} \right), & \text{for } \frac{a}{b} \geq \frac{1}{3} \end{cases} \quad \text{---- (5.19 B)}$$

Outlet

The momentum equation solver in Fluent uses a pressure correction method, which does not allow specification of two different reference pressures in the computational domain. Since the reactant gas flow channels are separate and generally at different pressures, pressure boundary conditions are used at the outlets.

Interface between the electrode and the flow channel

At the interface between the electrode and the flow channel, a user-defined function (UDF) was implemented to enforce a zero flux of electrons. This is done by overwriting the value of the potential in the first cell in the flow-channel side of the interface with the same value as the adjacent cell on the electrode side, thereby enforcing a zero potential gradient normal to the interface.

5.4 MATHEMATICAL MODEL

Useful work (electrical energy) is obtained from a fuel cell only when a current is drawn, but the actual cell potential (V_{cell}) is decreased from its equilibrium thermodynamic potential (E) because of irreversible losses. When current flows, a deviation from the thermodynamic potential occurs corresponding to the electrical work performed by the cell. The deviation from the equilibrium value is called the over potential and has been given the symbol (η). The over potentials originate primary from activation over potential (η_{act}), ohmic over potential (η_{ohmic}) and diffusion over potential (η_{diff}).

Therefore, the expression of the voltage of a single cell is

$$V_{cell} = E + \eta_{act} + \eta_{ohmic} + \eta_{diff} \quad \text{---- (5.21)}$$

The reversible thermodynamic potential of the chemical reactions, $H_2 + O_2$, previously described, is given by the equation:

$$E = E^0 - \left[\left(\frac{RT}{nF} \right) \ln \left(\frac{P_{H_2O}}{P_{H_2} \sqrt{P_{O_2}}} \right) \right] \quad \text{---- (5.22)}$$

Where the reversible standard potential E^0 of an electrochemical reaction is defined as

$$E^0 = - \frac{\Delta G^0}{nF} \quad \text{---- (5.23)}$$

Activation over potential arises from the kinetics of the charge transfer reaction across the electrode-electrolyte interface. In other words, a portion of the electrode potential is lost in driving the electron transfer reaction. Activation over potential is directly related to the nature of the electrochemical reactions and represents the magnitude of activation energy, when the reaction propagates at the rate demanded by the current. The activation over potential occurring at the electrodes of a PEMFC is given by Eq. (5.24), which is known as the Tafel equation.

$$\eta_{act} = \left(\frac{RT}{\alpha n F} \right) \ln(i_0) + \left(\frac{RT}{\alpha n F} \right) \ln(i) \quad \text{---- (5.24)}$$

Ohmic over potential results from electrical resistance losses in the cell. These resistances can be found in practically all fuel cell components: ionic resistance in the membrane, ionic and electronic resistance in the electrodes, and electronic resistance in the gas Diffusion backings, bipolar plates and terminal connections. This could be expressed using Ohm's Law equations such as

$$\eta_{ohmic} = -iR^{internal} \quad \text{---- (5.25)}$$

Diffusion over potential is caused by mass transfer limitations on the availability of the reactants near the electrodes. The electrode reactions require a constant supply of reactants in order to sustain the current flow.

When the diffusion limitations reduce the availability of a reactant, part of the available reaction energy is used to drive the mass transfer, thus creating a corresponding loss in output voltage. Similar problems can develop if a reaction product accumulates near the electrode surface and obstructs the diffusion paths or dilutes the reactants. The diffusion over potential can be expressed as

$$\eta_{diff} = \left(\frac{RT}{nF} \right) \ln \left(\frac{i_1 - i}{i_1} \right) \quad \text{---- (5.26)}$$

The thermodynamic efficiency of the fuel cell E_{fc} can be determined as the ratio of output work rate W_{gross} to the product of the hydrogen consumption rate \dot{m}_{H_2} and the lower heating value of hydrogen LHV_{H_2}

$$E_{fc} = \frac{W_{gross}}{\dot{m}_{H_2} \cdot LHV_{H_2}} \quad \text{---- (5.27)}$$

Once the output voltage of the stack is determined for a given output current, the gross output power is found as:

$$W_{gross} = I \cdot V_{cell} \quad \text{---- (5.28)}$$

The output current is correlated with the hydrogen mass flow rate by the equation

$$\dot{m}_{H_2} = \frac{I \cdot MW_{H_2}}{2 F} \quad \text{---- (5.29)}$$

Thus, the thermodynamic efficiency of the fuel cell can be simplified as follows:

$$E_{fc} = \frac{2V_{cell}F}{MW_{H_2} \cdot LHMV_{H_2}} \quad \text{---- (5.30)}$$

5.5 PHYSICAL PROPERTIES AND OPERATING PARAMETERS OF PEM FUEL CELL

The geometry, parameters and operating conditions used in the simulations are listed in the tables. This is not a very satisfactory way of verifying model performance. Until progress is made in the difficult problem of obtaining detailed and reliable, we will continue to use polarization curves and complement the assessment with an analysis of the physical results obtained with the model. Given the state of development of PEM fuel cell modeling, the complexity of the transport phenomena, and the large range of physical scales involved, and the uncertainty in determining some of the physico-chemical parameters, it is any case unrealistic to expect accurate quantitative agreement between mathematical and computational model simulations.

Simulation based on physically representative models should however yield correct relative trends and provide valuable insight and guidance for design and optimization. The geometry of the fuel cell simulated in this work is a straight section consisting of bipolar plates with flow channels separated by a membrane-electrode assembly.

Another reason for the improved performances is the partial pressure increase in the reactant gases with increasing operating pressure. Changes in operating pressure have a large impact on the inlet composition and hence on the current density, as shown in Figure 5.5. The maximum current density shifts positively with increasing pressure because the rate of the chemical reaction is proportional to the partial pressures of the hydrogen and oxygen. Thus, the effect of increased pressure is most prominent when using air. In essence, higher pressures help to force the hydrogen and oxygen into contact with the electrolyte. This sensitivity to pressure is greater at high currents.

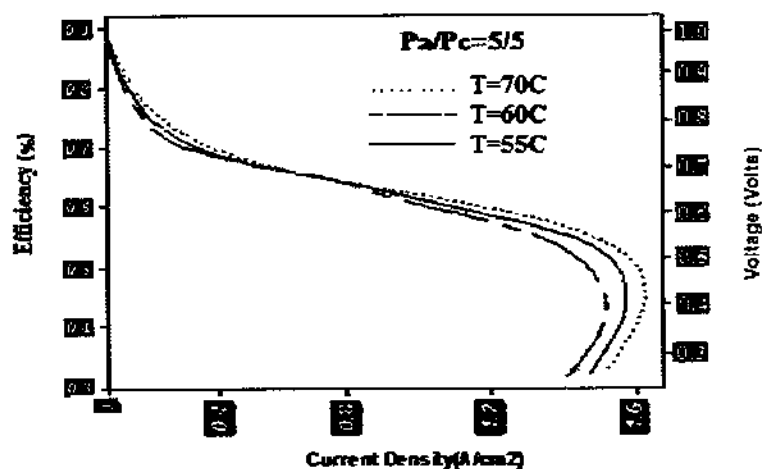


FIGURE 5.4 RELATIONSHIPS BETWEEN CURRENT DENSITY, VOLTAGE AND EFFICIENCY FOR DIFFERENT TEMPERATURE

The fuel cell efficiency is directly proportional to the cell potential; therefore, efficiency is also a function of current density. Figures 5.4 and 5.5, therefore, have both voltage and efficiency on the “y” axis. The efficiency at maximum power is much lower than that at partial loads, which makes the fuel cells very attractive and efficient for applications with highly variable loads where most of the time the fuel cell is operated at low load and high efficiency. The fuel cell's nominal efficiency is therefore an arbitrary value, ranging anywhere between 0.3 and 0.6, which can be selected for any fuel cell based on economic rather than on physical constraints.

For example, for a fuel cell at a reactant pressure of 1 atm and 72^oC cell temperature, one may select a maximum operating point at 0.5 V and 0.89 A/cm², resulting in 0.44 W/cm² and an efficiency of 0.4. However, one may get the same

power output by selecting 2 cells, connected in series, operating at 0.71 V and 0.31 A/cm² each. Obviously, the latter would be twice as expensive, but it would be more efficient (0.57), and therefore would consume less fuel. This example clearly illustrates that the efficiency of a fuel cell may be “bought” by adding more cells, and it is driven by economic factors, such as the cost of individual cells, cost of hydrogen and the resulting cost of generated power.

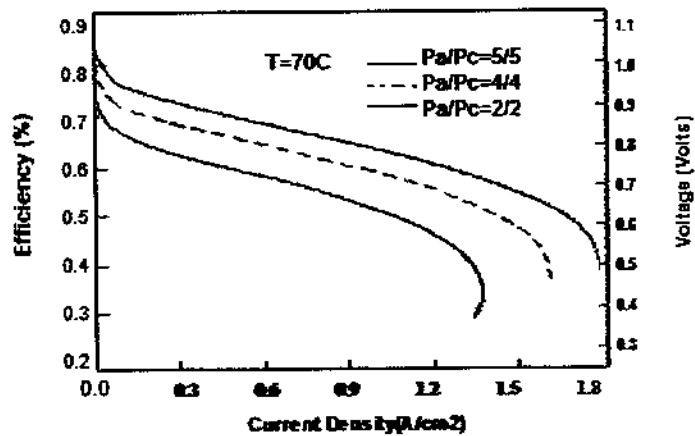


FIGURE 5.5 RELATIONSHIPS BETWEEN CURRENT DENSITY, VOLTAGE AND EFFICIENCY FOR DIFFERENT PRESSURE

Returning to Figures 5.4 and 5.5, the maximum power occurs at approximately 0.4 to 0.5 V, which corresponds to a relatively high current. At the peak point, the internal resistance of the cell is equal to the electrical resistance of the external circuit. However, since efficiency drops with increasing voltage, there is a tradeoff between high power and high efficiency. Fuel cell system designers must select the desired operating range according to whether efficiency or power is paramount for the given application.

6.3 BOUNDARY CONDITIONS

The boundary conditions are specified in gambit. Boundary conditions pressure inlet, porous jump, and outflow are shown in Figure 6.4. The pressure inlet and outflow are given in anode and cathode flow channel surfaces. Porous jump is given in electrodes, catalyst and membrane surfaces. Other surfaces are specified as wall.

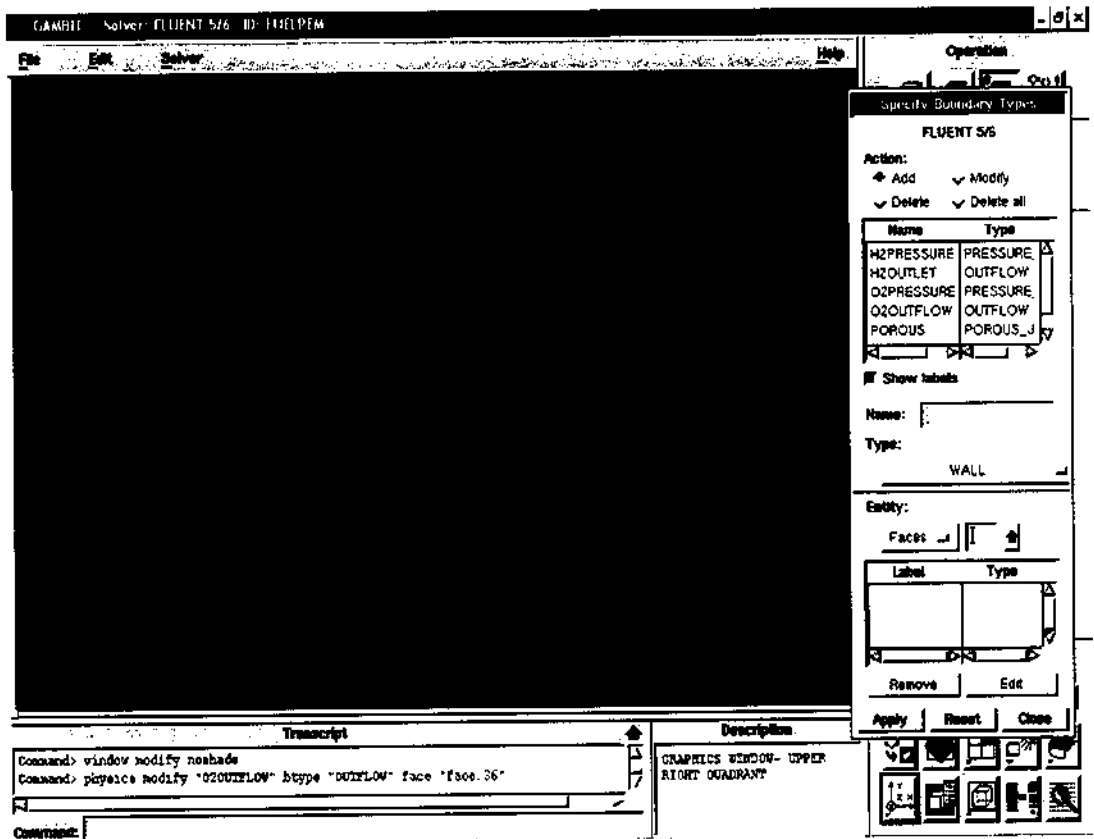


FIGURE 6.4 BOUNDARY CONDITIONS

6.2 MESHING

Volumetric mesh is created using meshing option. The Figure 6.2 and 6.3 shows partially meshed model and fully meshed model. Fluent5/6 solver is taken for solving the meshed model.

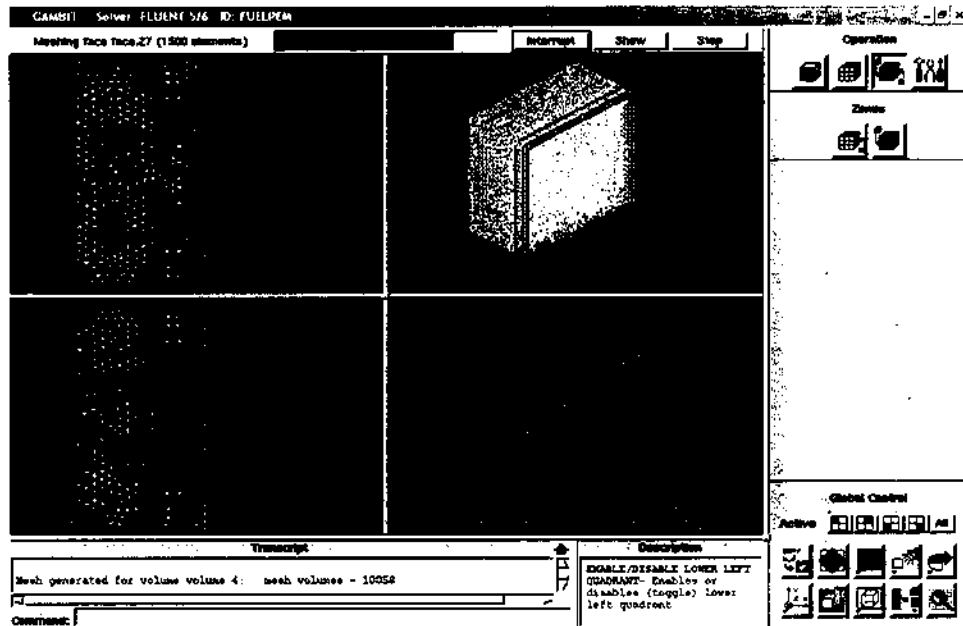


FIGURE 6.2 PARTIALLY MESHED MODEL

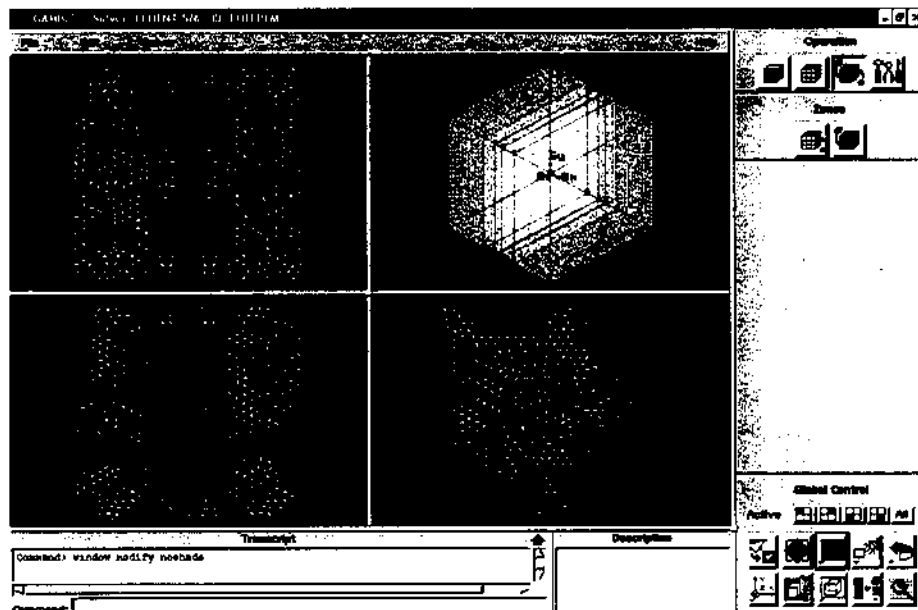


FIGURE 6.3 FULLY MESHED MODEL

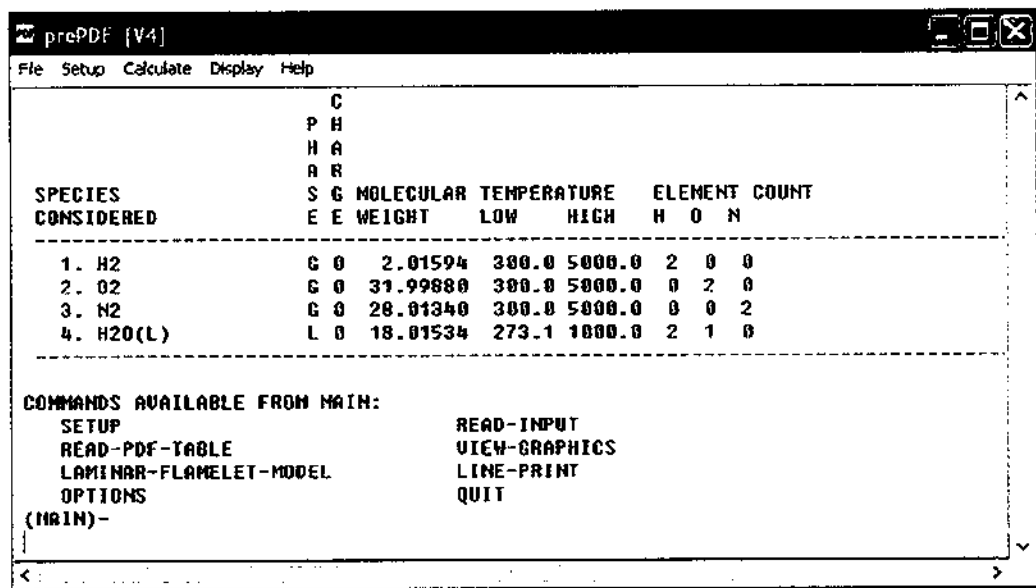
6.4 INITIAL CONDITIONS

PrePDF is used to apply initial conditions. The initial conditions are like number of species used, operating parameters.

When you use the mixture-fraction/PDF model, you begin by preparing a PDF file with the preprocessor, PrePDF. The PDF file contains look-up tables relating species concentrations and temperatures to the mixture fraction.

The look-up tables are used by FLUENT to obtain these scalars during the solution procedure. After creating the PDF file, you will activate the PDF modeling option in FLUENT and define boundary conditions for the mixture fraction and its variance. You will then solve the problem in the usual manner, using the PDF file to describe the system chemistry.

The Figure 6.5 shows the chemical species (fuel, oxidizer and the products) of this process. Fuel used is Hydrogen, oxidizer is air (contains Nitrogen and Oxygen) and the product is water.



SPECIES CONSIDERED	S E	G E	MOLECULAR WEIGHT	TEMPERATURE		ELEMENT COUNT		
				LOW	HIGH	H	O	N
1. H2	G	0	2.01594	300.0	5000.0	2	0	0
2. O2	G	0	31.99880	300.0	5000.0	0	2	0
3. N2	G	0	28.01340	300.0	5000.0	0	0	2
4. H2O(L)	L	0	18.01534	273.1	1000.0	2	1	0

COMMANDS AVAILABLE FROM MAIN:

SETUP	READ-INPUT
READ-PDF-TABLE	VIEW-GRAPHICS
LAMINAR-FLAMELET-MODEL	LINE-PRINT
OPTIONS	QUIT

(MAIN)-

FIGURE 6.5 SPECIES PROPERTIES

The Figure 6.6 shows operating temperature of this process. From the mathematical model optimum operating characters are taken for analysis.

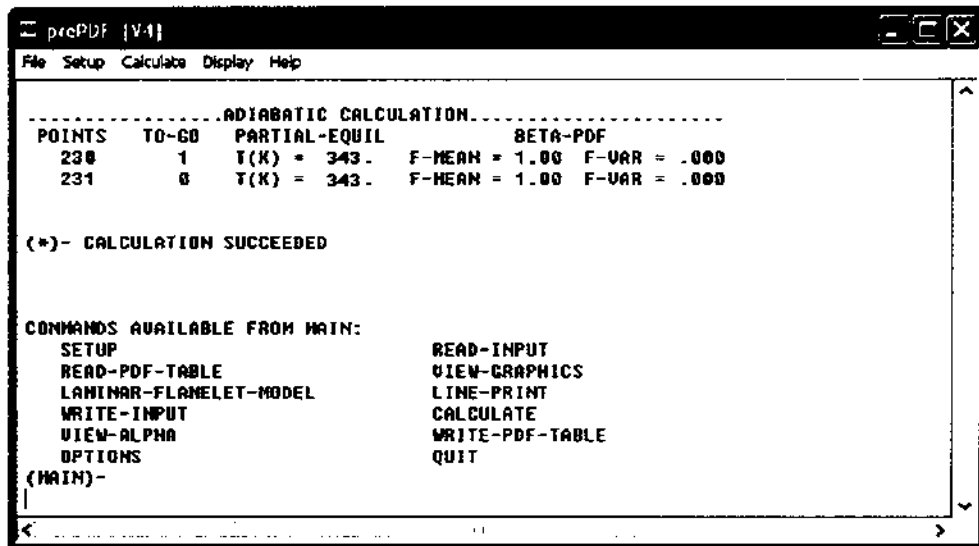


FIGURE 6.6 OPERATING TEMPERATURE

The Figure 6.7 shows the species composition. The figure shows the relation between the Mole fraction and mixture fraction.

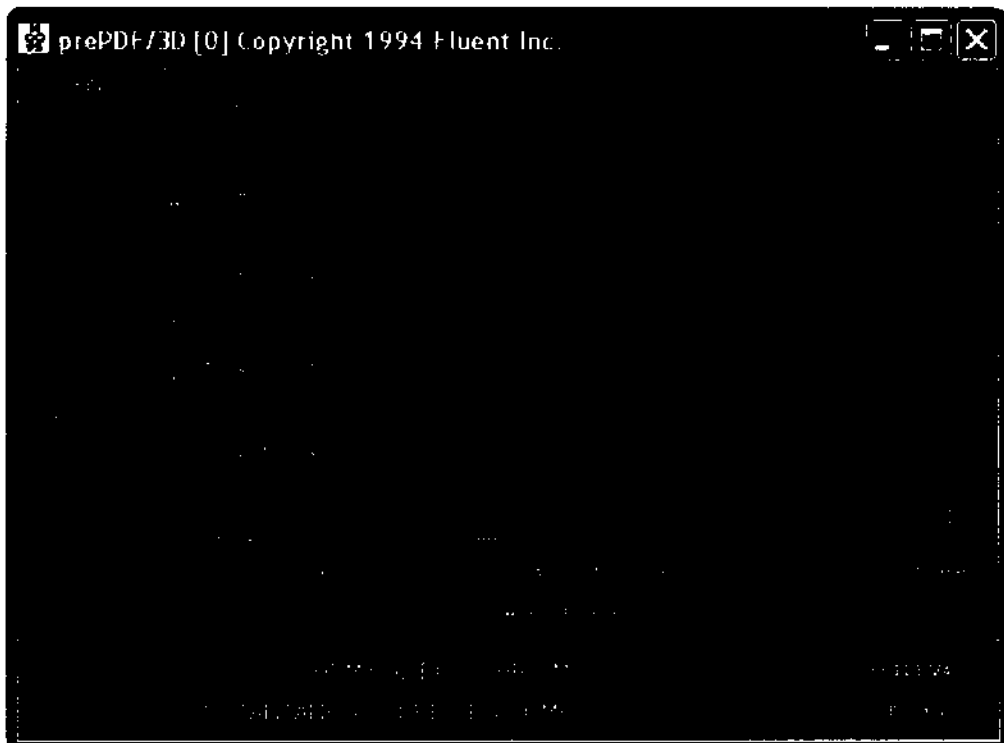
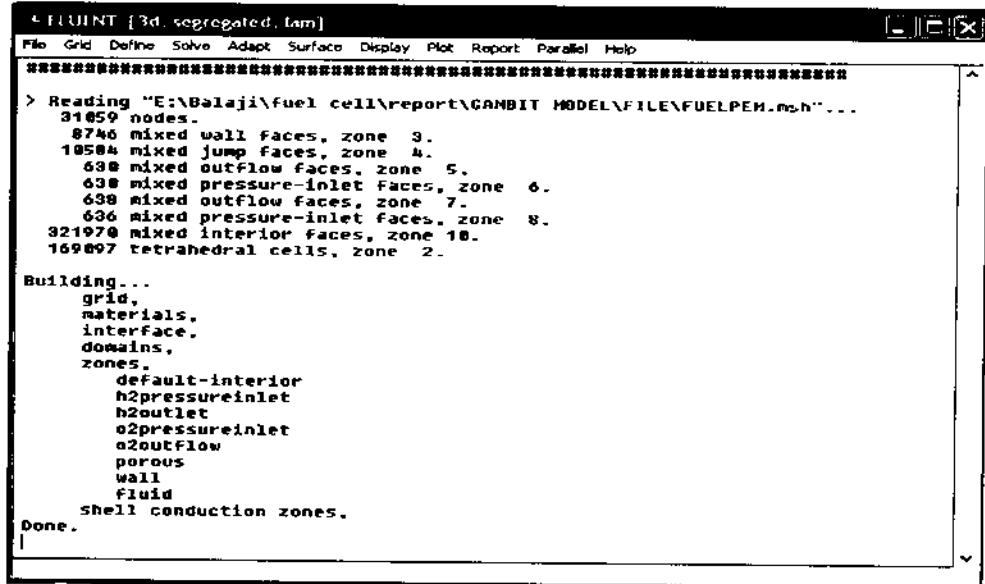


FIGURE 6.7 SPECIES COMPOSITION

6.5 GRID CHECK

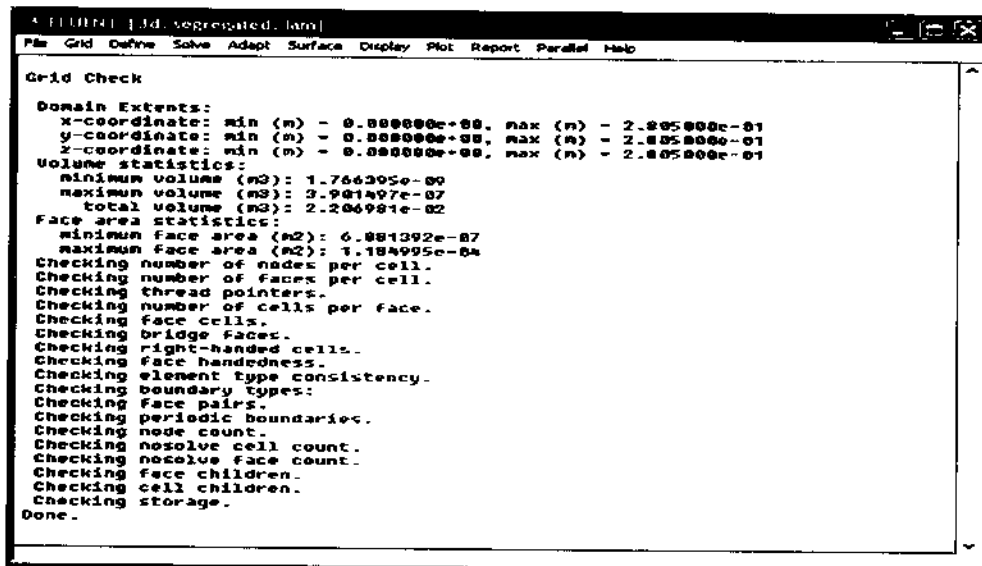
The Figure 6.8 shows the data of mesh file read from Gambit to Fluent. It shows the flow fields in the cell and the number of nodes generated in the meshed model.



```
4 FLUENT [3d, segregated, lam]
File Grid Define Solve Adapt Surface Display Plot Report Parallel Help
> Reading "E:\Balaji\fuel cell\report\GAMBIT MODEL\FILE\FUELPEM.msh"...
31659 nodes.
8746 mixed wall faces, zone 3.
10584 mixed jump faces, zone 4.
638 mixed outflow faces, zone 5.
438 mixed pressure-inlet faces, zone 6.
638 mixed outflow faces, zone 7.
636 mixed pressure-inlet faces, zone 8.
321970 mixed interior faces, zone 10.
169097 tetrahedral cells, zone 2.
Building...
grid,
materials,
interface,
domains,
zones.
default-interior
h2pressureinlet
h2outlet
o2pressureinlet
o2outflow
porous
wall
fluid
shell conduction zones.
Done.
```

FIGURE 6.8 READING MESH FILE

The Figure 6.9 shows the grid check on the meshed model. The grid check process was taken successfully and there is no error in the meshed model.



```
4 FLUENT [3d, segregated, lam]
File Grid Define Solve Adapt Surface Display Plot Report Parallel Help
Grid Check
Domain Extents:
x-coordinate: min (m) = 0.000000e+00, max (m) = 2.005000e-01
y-coordinate: min (m) = 0.000000e+00, max (m) = 2.005000e-01
z-coordinate: min (m) = 0.000000e+00, max (m) = 2.005000e-01
Volume statistics:
minimum volume (m3): 1.764305e-09
maximum volume (m3): 3.901497e-07
total volume (m3): 2.204981e-02
Face area statistics:
minimum face area (m2): 6.881392e-07
maximum face area (m2): 1.184995e-04
Checking number of nodes per cell.
Checking number of faces per cell.
Checking thread pointers.
Checking number of cells per face.
Checking face cells.
Checking bridge faces.
Checking right-handed cells.
Checking face handedness.
Checking element type consistency.
Checking boundary types.
Checking face pairs.
Checking periodic boundaries.
Checking node count.
Checking nosolve cell count.
Checking nosolve face count.
Checking face children.
Checking cell children.
Checking storage.
Done.
```

FIGURE 6.9 GRID CHECK

6.6 ITERATION PROCESS

After giving the conditions in fluent iteration process is taken out. The Figure 6.10 shows relation between the iterations and various residuals.

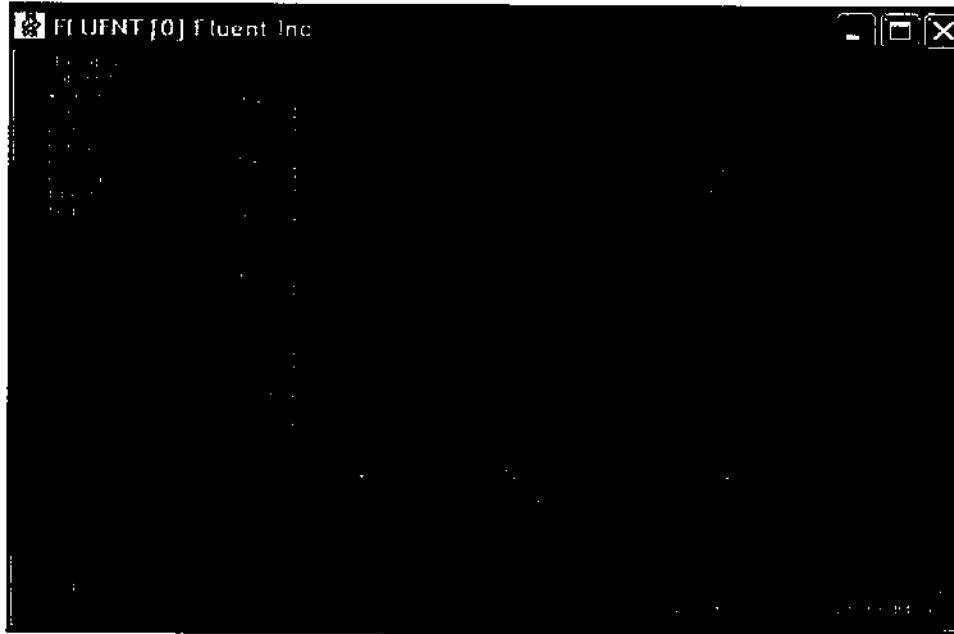


FIGURE 6.10 SCALED RESIDUALS

The Figure 6.11 shows that there is no incomplete particle in the analysis process. The iteration process is converged at 320th iteration.

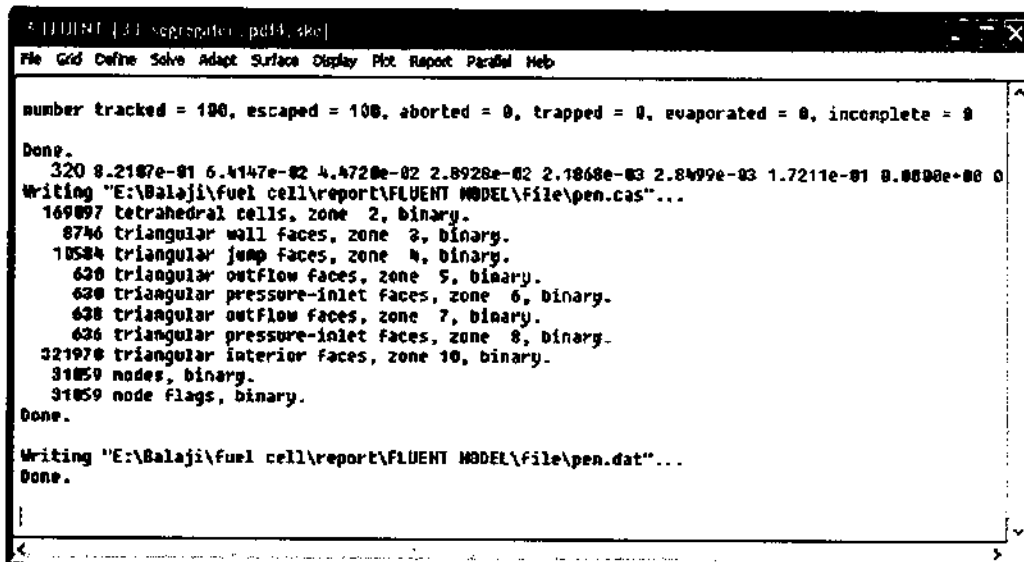


FIGURE 6.11 ITERATION PROCESS

CHAPTER 7

*RESULTS AND
DISCUSSIONS*

The various results are obtained from the analysis of fuel flow in the fuel cell is discussed in this chapter. The results are pressure, density, velocity magnitude and turbulent kinetic energy.

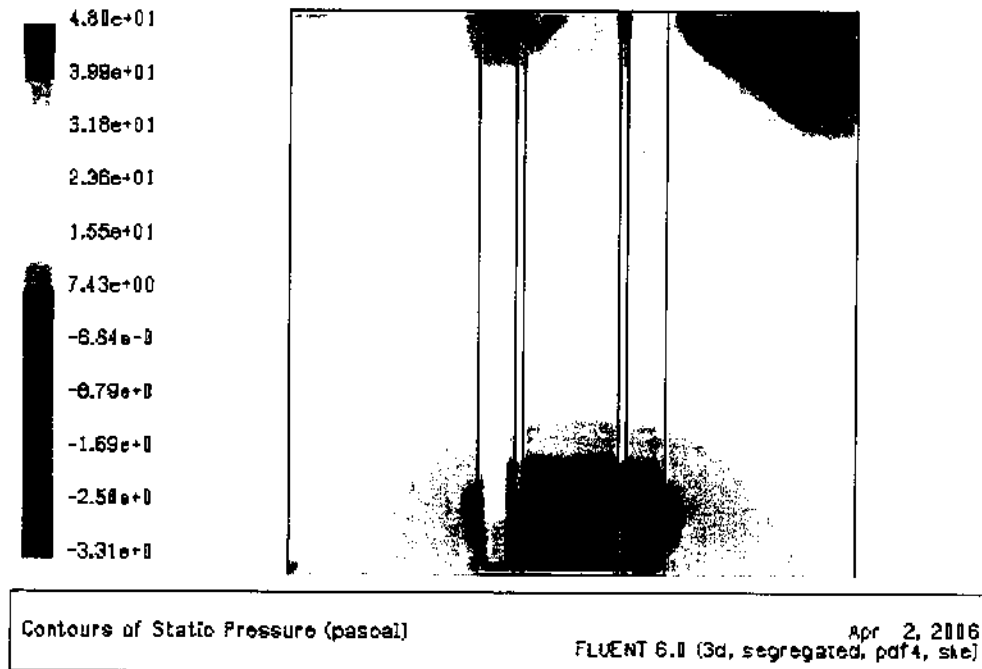


FIGURE 7.1 CONTOURS OF STATIC PRESSURE

The Figure 7.1 shows the contours of pressure of the fluid inside the fuel cell. Pressure is evenly distributed through the cell volumes.

The Figure 7.2 shows the density of fluid in the cell including the walls of the cell. It shows the density at the walls.

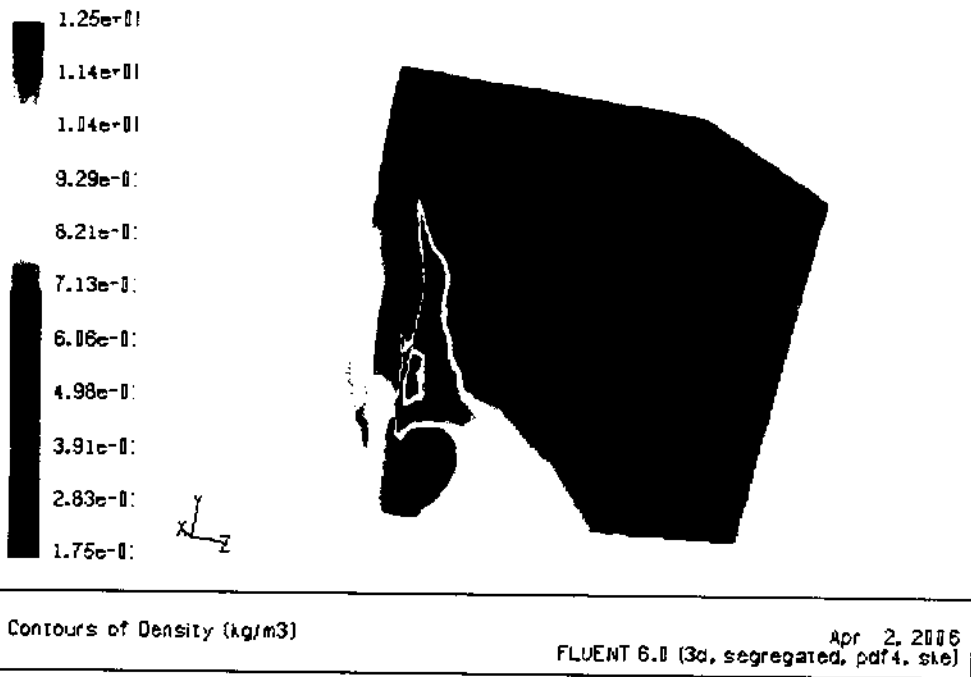


FIGURE 7.2 DENSITY OF FLUID IN CELL

The Figure 7.3 shows the density of fluid in flow volume. Flow volume has inner surfaces of the cell not the walls.

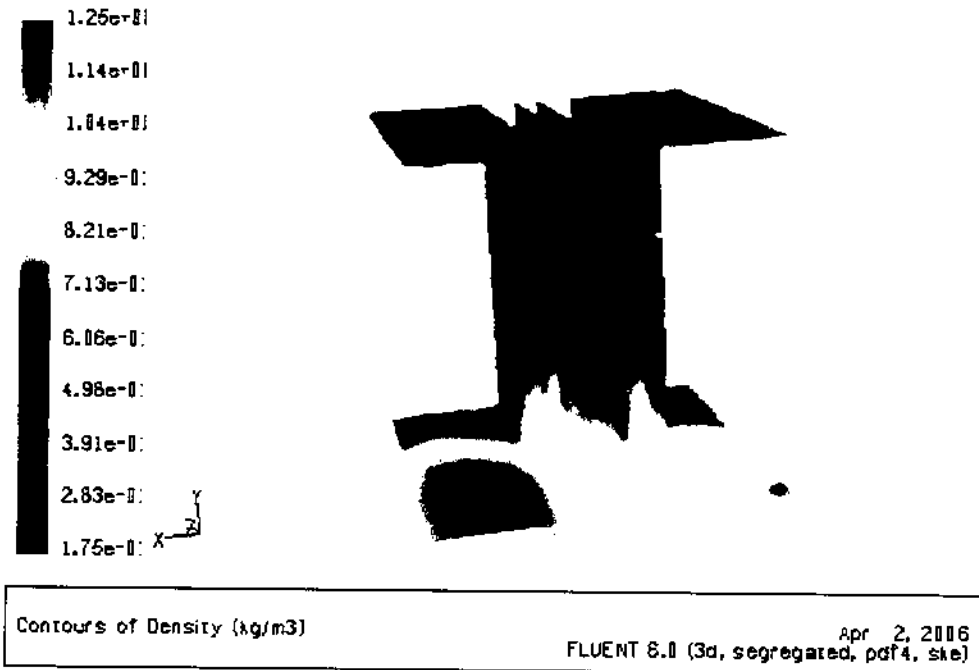


FIGURE 7.3 DENSITY OF FLUID IN FLOW VOLUME

The Figure 7.4 shows the velocity in flow volume of the cell. Velocity magnitude is more at inlet and minimum at outlet. Velocity is gradually decreasing from inlet to outlet.

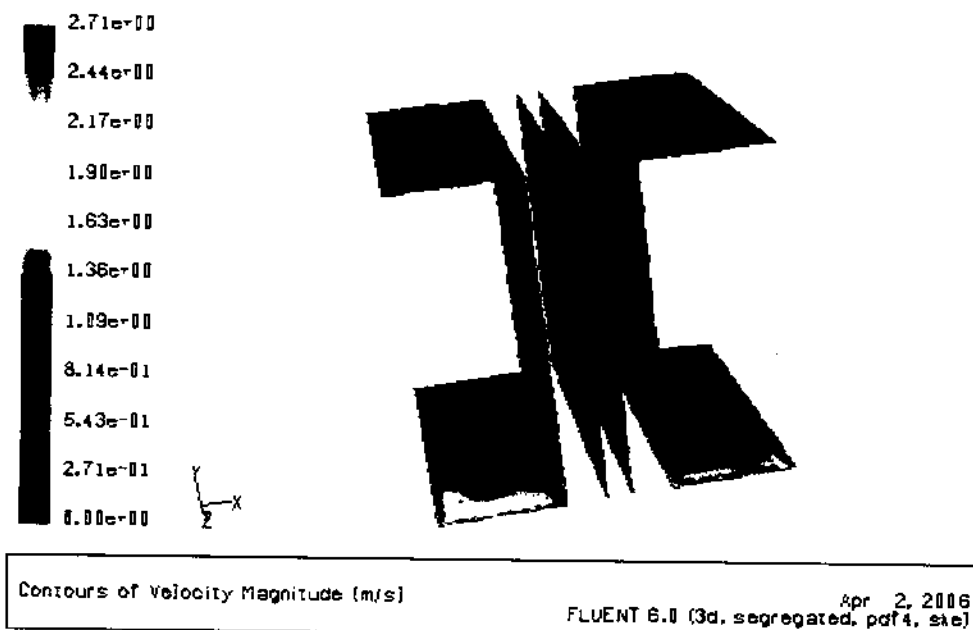


FIGURE 7.4 VELOCITY

The Figure 7.5 shows that how the turbulent kinetic energy taken place inside the cell. It shows that turbulence is more or less same with in the cell.

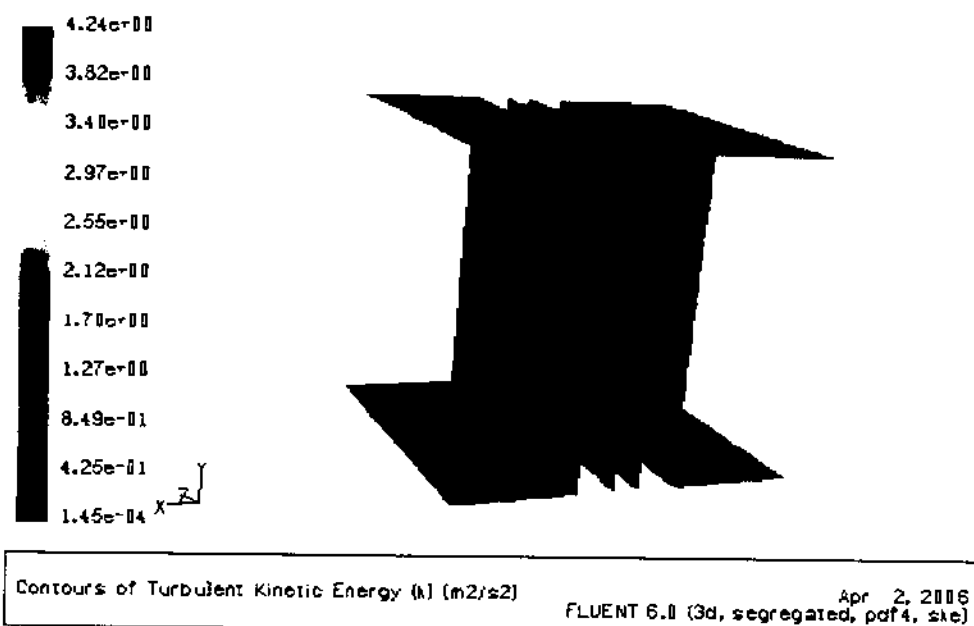


FIGURE 7.5 TURBULENT KINETIC ENERGY

A mathematical model based on physical-chemical knowledge of the phenomena occurring inside the cell of a PEMFC has been developed and the effect of operation conditions on cell performance is investigated.

The effect of temperature on the inlet gas composition is particularly strong in the pressure ranges from 2-to 4 atm. In 5 atm pressure the composition changes only slightly with pressure. Changes in operating pressure have a large impact on the inlet composition and, hence, on fuel cell performance.

For steady operation, a fuel cell does not have to be operated at its maximum power, where the efficiency is lowest. When a higher nominal cell potential is selected, savings on fuel cost offsets the cost of additional cells.

The results of the present study indicate that operating temperature and pressure can be optimized, based on cell performance, for given design and other operating conditions.

CHAPTER 8

CONCLUSIONS

REFERENCES

1. Barbir.F., and Gomez.T. (1997), Efficiency and Economics of Proton Exchange Membrane (PEM) Fuel Cells, *International Journal of Hydrogen Energy*, 22, p.p.1027-1037.
2. Ben Kenney, Kunal Karan (2004), *Mathematical Micro-Model of a Solid Oxide Fuel Cell Composite Cathode*, Fuel Cell Research Centre, Canada.
3. Berning, T. and Djinali, N. (2003), Three-dimensional Computational Analysis of Transport Phenomena in a PEM Fuel Cell-a Parametric Study, *Journal of Power Sources*, p.p. 440-452.
4. Brenda L.Garcia, Vijay A. Sethuraman, John W. Weidner and Ralph E. White (2004), Mathematical Model of a Direct Methanol Fuel Cell, *Journal of Fuel Cell Science and Technology*, p.p.123-137.
5. Cownden, R., Nahon, M. and Rosen, M.A. (2001), Modeling and Analysis of a Solid Polymer Fuel Cell System for Transportation Applications, *International Journal of Hydrogen Energy*, 26, p.p.615-623.
6. Johnson, R., Morgan, C., Witmer, D. and Johnson, T. (2001), Performance of a Proton Exchange Membrane Fuel Cell Stack, *International Journal of Hydrogen Energy*, 26, p.p.879-887.
7. Mann, R.F., Amphlett, J.C., Hooper, M.A, Jensen, H.M., Peppley, B.A. and Roberge, P.R. (2000), Development and Application of a Generalised Steady-State Electrochemical Model for a PEM Fuel Cell, *Journal of Power Sources*, 86, p.p.173-180.
8. Marco Mulas, Giovanni Murgia, Lorenga Pisani and Rosaria Russo (2002), *A quasi-3D Computer model of a Planar Solid-Oxide Fuel Cell Stack*, Energy and Process Engineering Department. Italy.
9. McGarry, M. and Grega, L. (2005), Effects of Inlet Flow Distribution and Magnitude on Reactant Distribution for PEM Fuel Cells, *Journal of Fuel Cell Science and Technology*, p.p.92-105.
10. McLean, G.F. Niet, T. Prince-Richard, S. and Djilali, N. (2002), An Assessment of Alkaline Fuel Cell Technology, *International Journal of Hydrogen Energy*, pp.507-526.
11. Qingyun Liu and Junxiao Wu (2005), Multi-Resolution PEM Fuel Cell Model Validation and Accuracy Analysis, *Journal of Fuel Cell Science and Technology*, p.p.55-68.

12. Sandip Pasricha and Steven R. Shaw (2004), *A Dynamic PEM Fuel Cell Model*, IEEE Transaction on Energy Conversion.
13. Saptarshi Bas, Hang Xu, Michel W. Renfro and Baki M. Cetegen (2005), In Situ Optical Diagnostics for Measurements of Water Vapor Partial Pressure in a PEM Fuel Cell, *Journal of Fuel Cell Science and Technology*, p.p.78-90.
14. Sivertsan, B.R. and Djilali, N. (2005), CFD-based Modeling of Proton Exchange Membrane Fuel Cells, *Journal of Power Sources*, p.p.65-78.